Supporting Information

Synthesis, structure and reactivity of guanidinate rare earth metal bis(*o*-aminobenzyl) complexes

Feng Kong,[a] Meng Li[a], Xigeng Zhou[a] and Lixin Zhang[a*]

Contents

NMR spectra of all complexes (Except for **2c**, **3c**, **4c** and **5c**) (Page 2-15)

NMR spectra of representative PIP (Page 16-17)

GPC curves of PIP obtained by complex **2a**/$[Ph_3C][B(C_6F_5)_4]$ binary system (Page 18)

Molecular structure of **3b-d**, **4c**, **4d**, **5c** and **5d** (Page 19-23)

Cryatallographic data and structure refinement details of **1**, **3b-d**, **4c**, **4d**, **5c** and **5d** (Page 24-25)

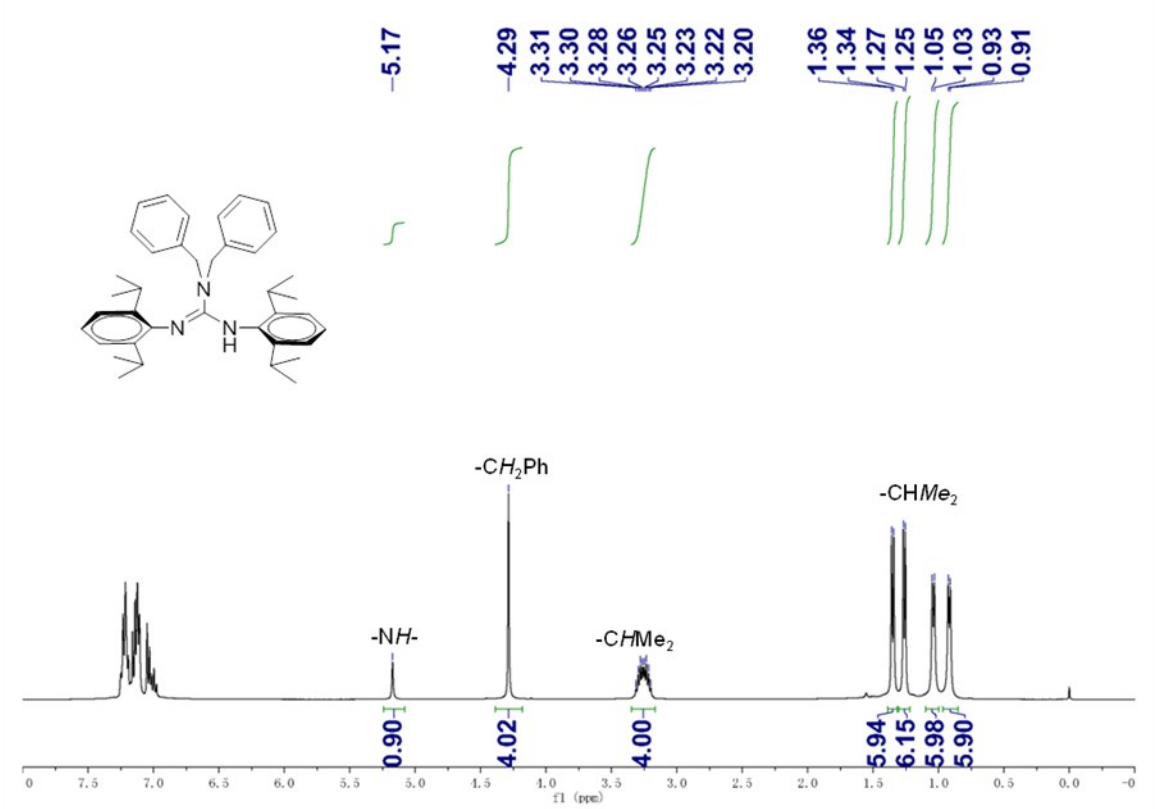

Figure S1. ^{1}H NMR spectrum of **1** obtained in $CDCl_3$ at room temperature.

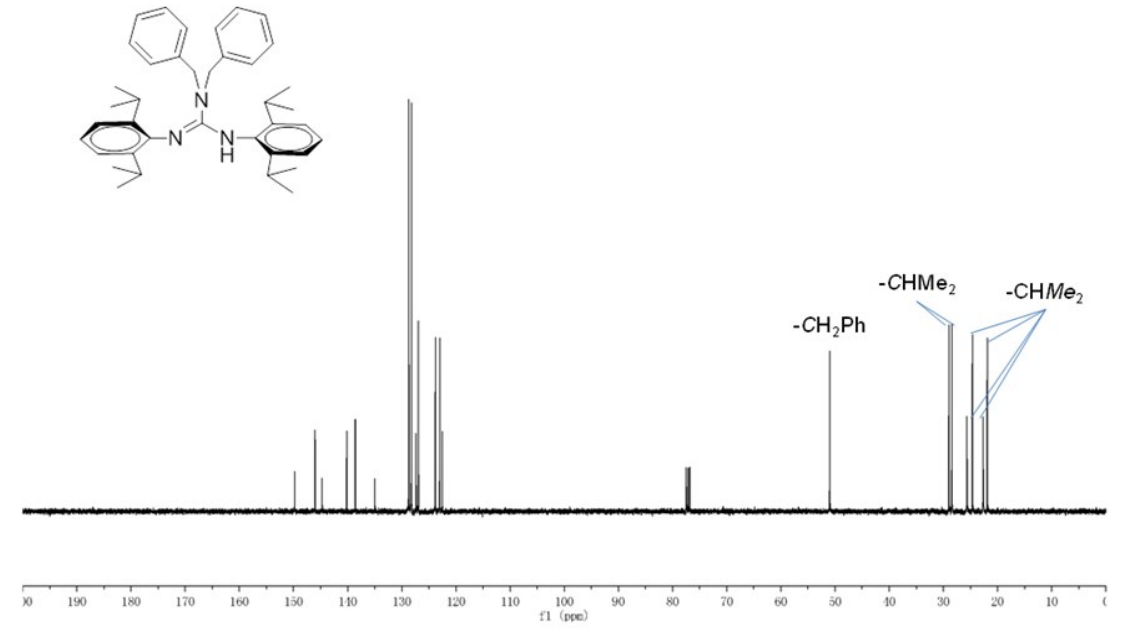

Figure S2. ^{13}C NMR spectrum of **1** obtained in $CDCl_3$ at room temperature.

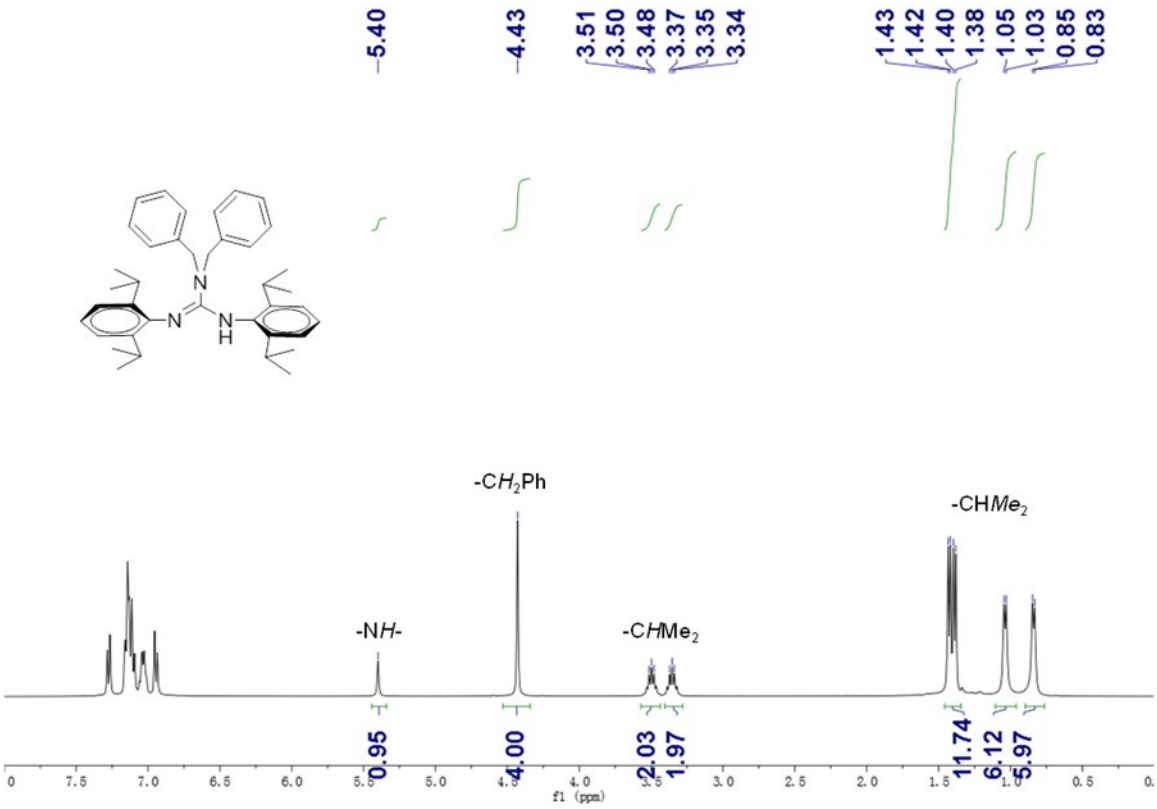

Figure S3. ^{1}H NMR spectrum of **1** obtained in C_6D_6 at room temperature.

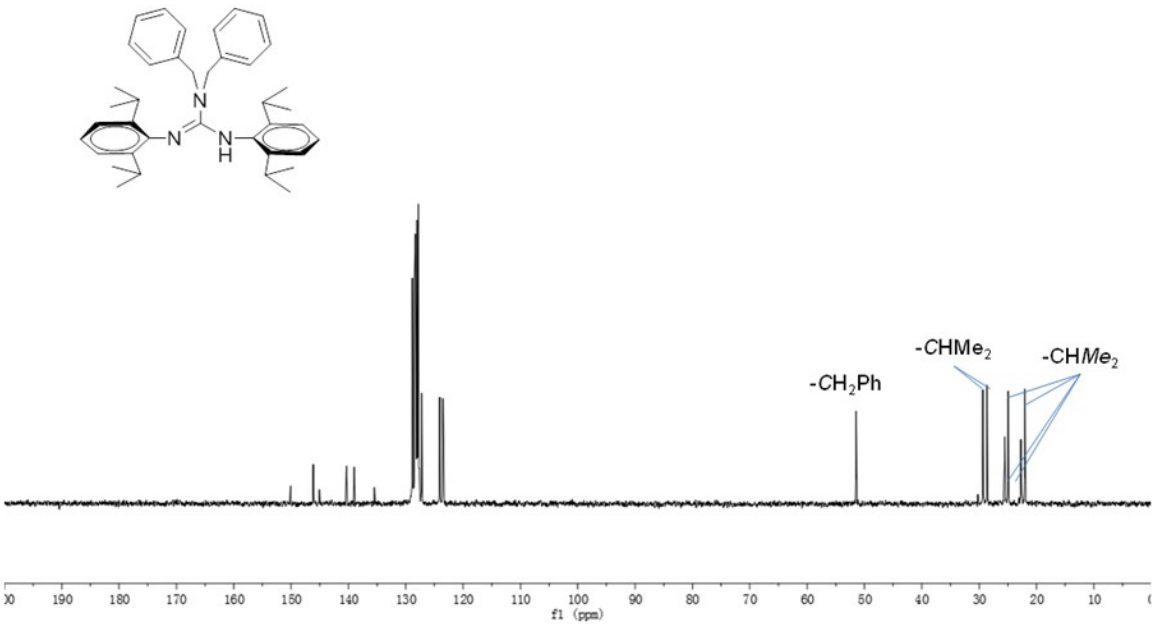

Figure S4. ^{13}C NMR spectrum of **1** obtained in C_6D_6 at room temperature.

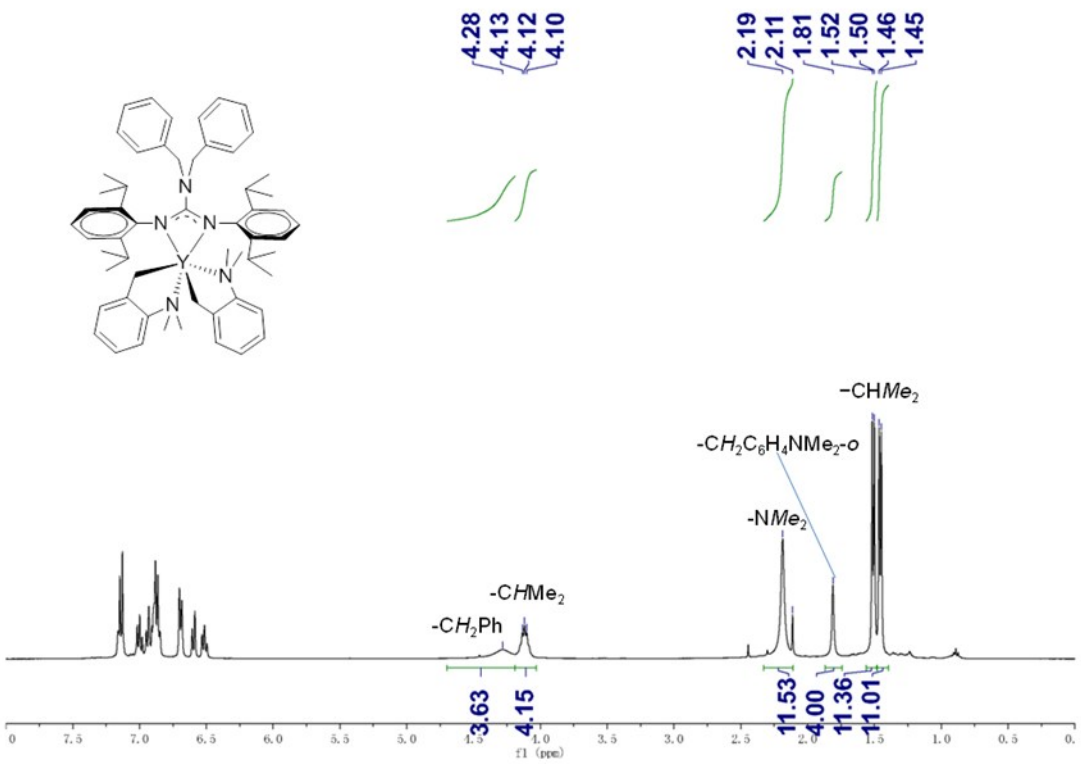

Figure S5. ^{1}H NMR spectrum of **2a** obtained in C_6D_6 at room temperature.

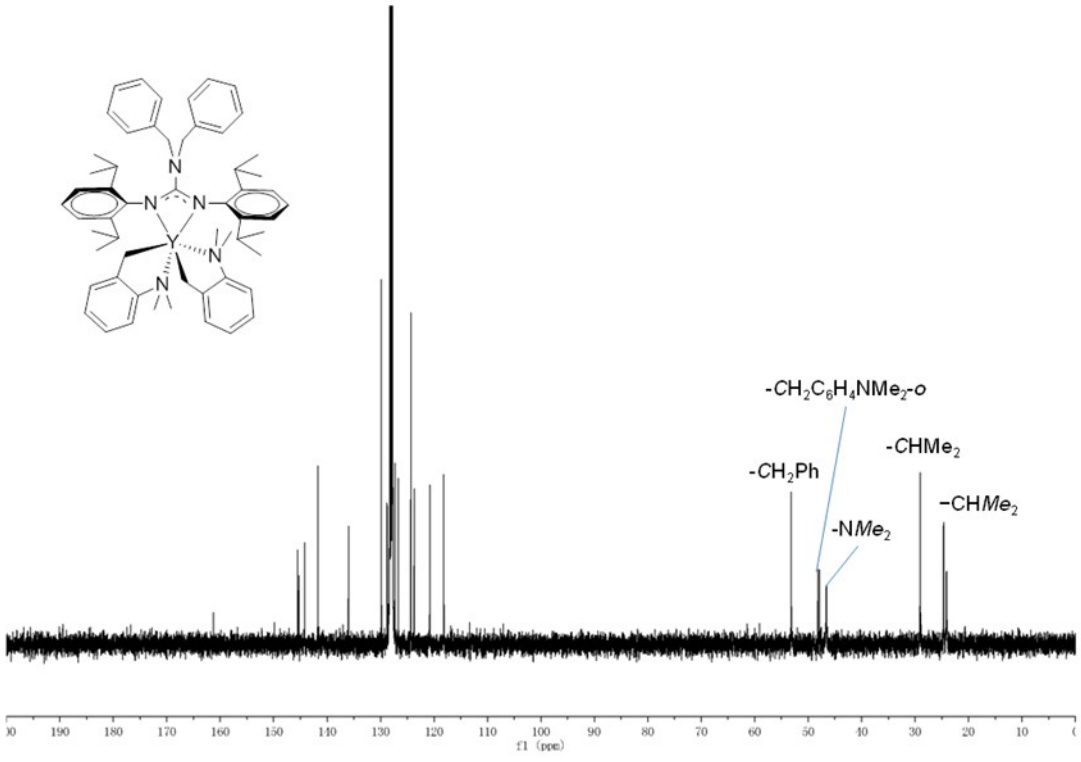

Figure S6. ^{13}C NMR spectrum of **2a** obtained in C_6D_6 at room temperature.

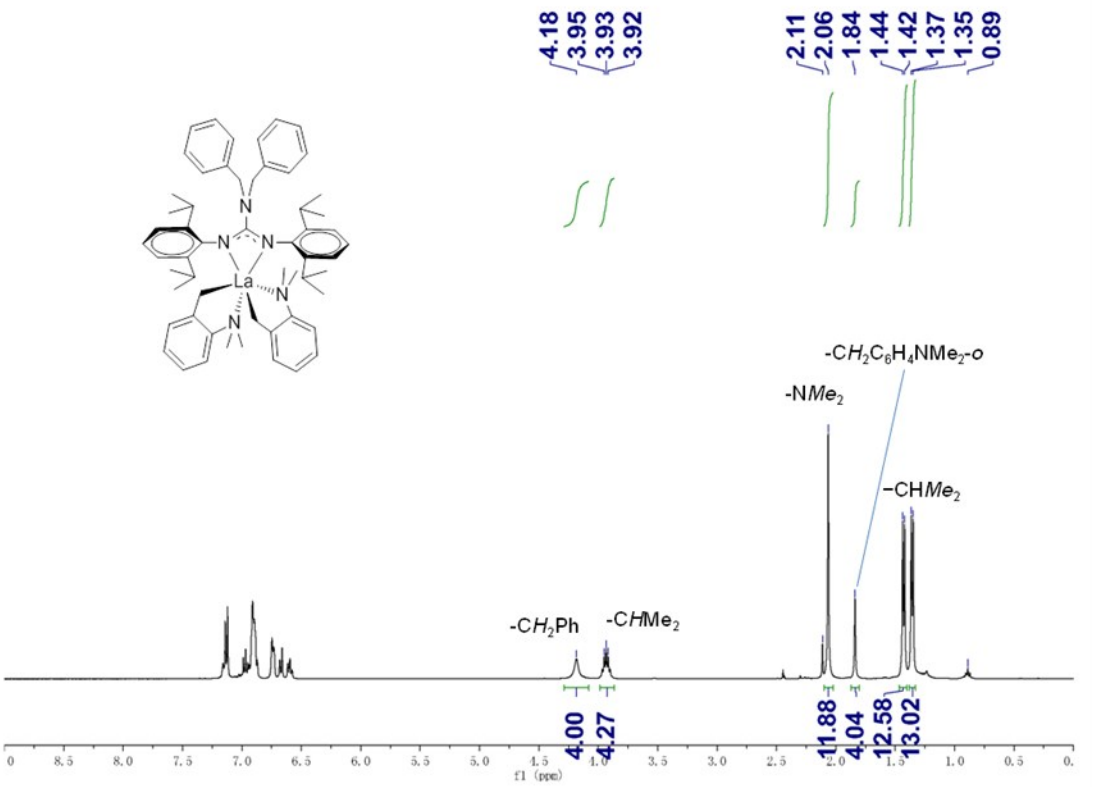

Figure S7. ^{1}H NMR spectrum of **2b** obtained in C_6D_6 at room temperature.

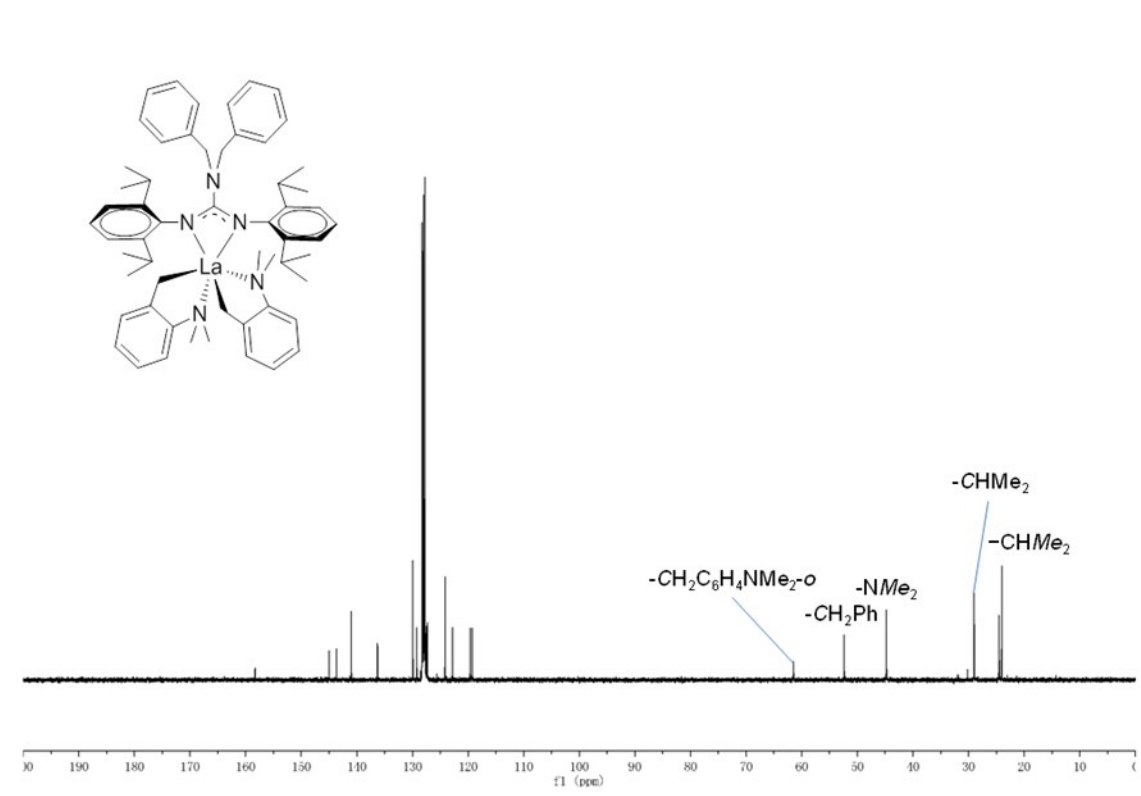

Figure S8. ^{13}C NMR spectrum of **2b** obtained in C_6D_6 at room temperature.

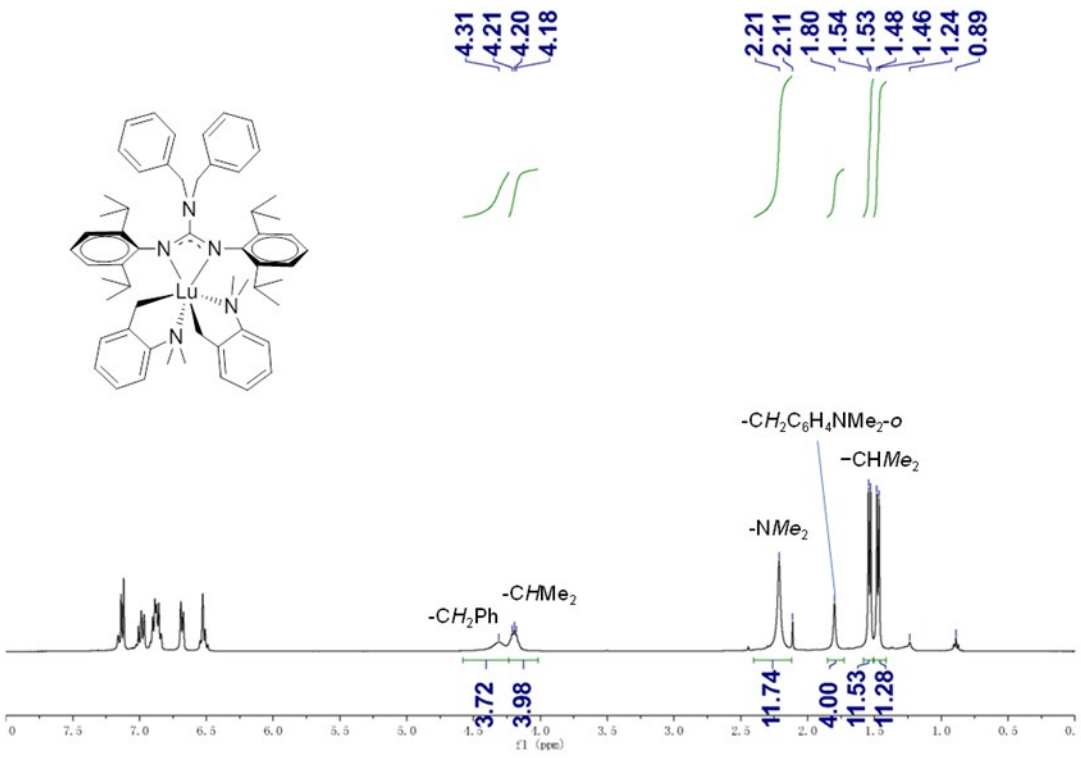

Figure S9. ^{1}H NMR spectrum of **2d** obtained in C_6D_6 at room temperature.

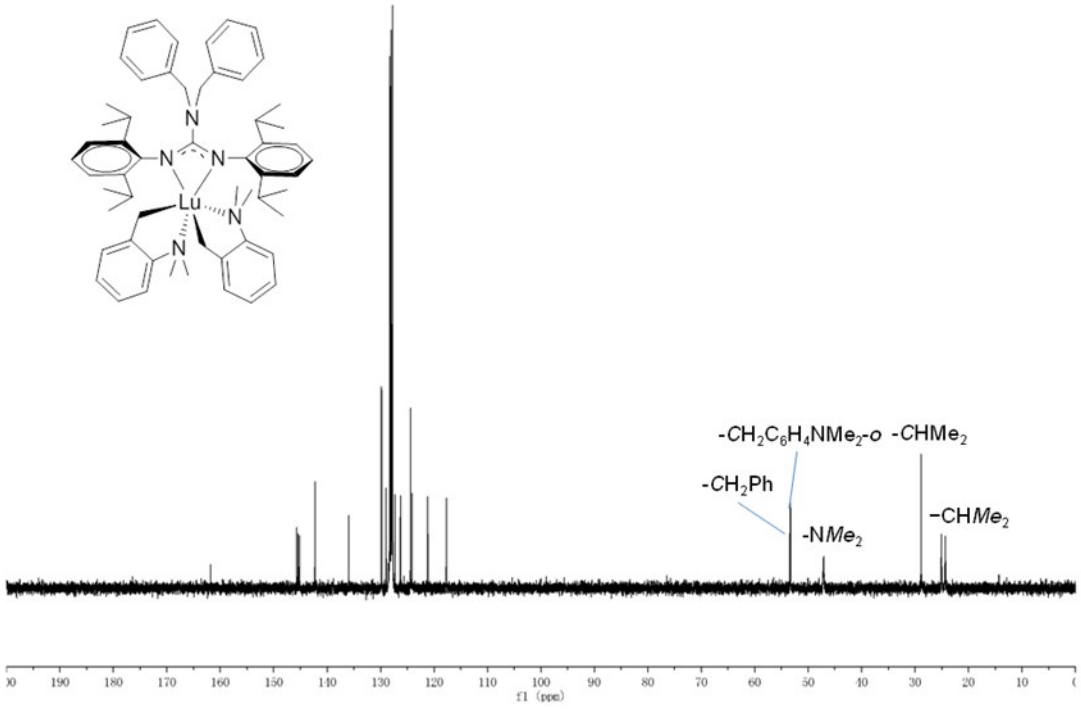

Figure S10. ^{13}C NMR spectrum of **2d** obtained in C_6D_6 at room temperature.

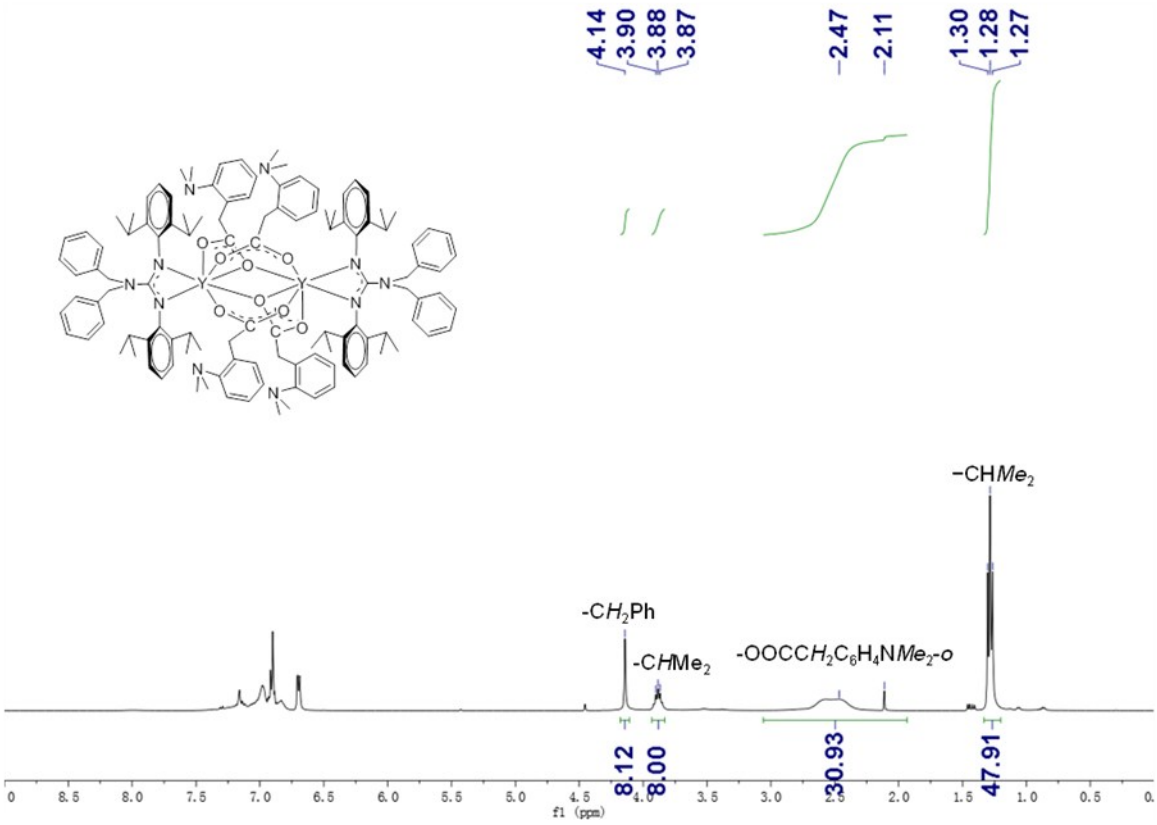

Figure S11. ^{1}H NMR spectrum of **3a** obtained in C_6D_6 at room temperature.

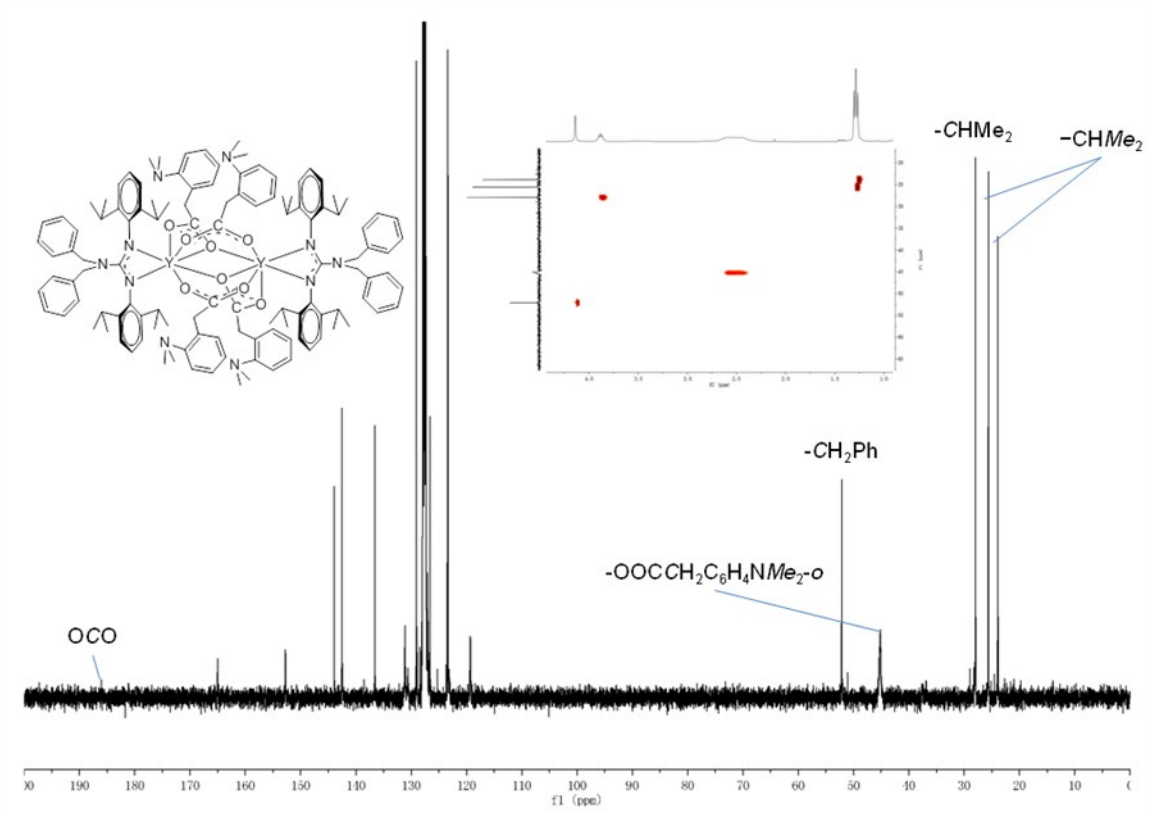

Figure S12. ^{13}C NMR spectrum of **3a** obtained in C_6D_6 at room temperature.

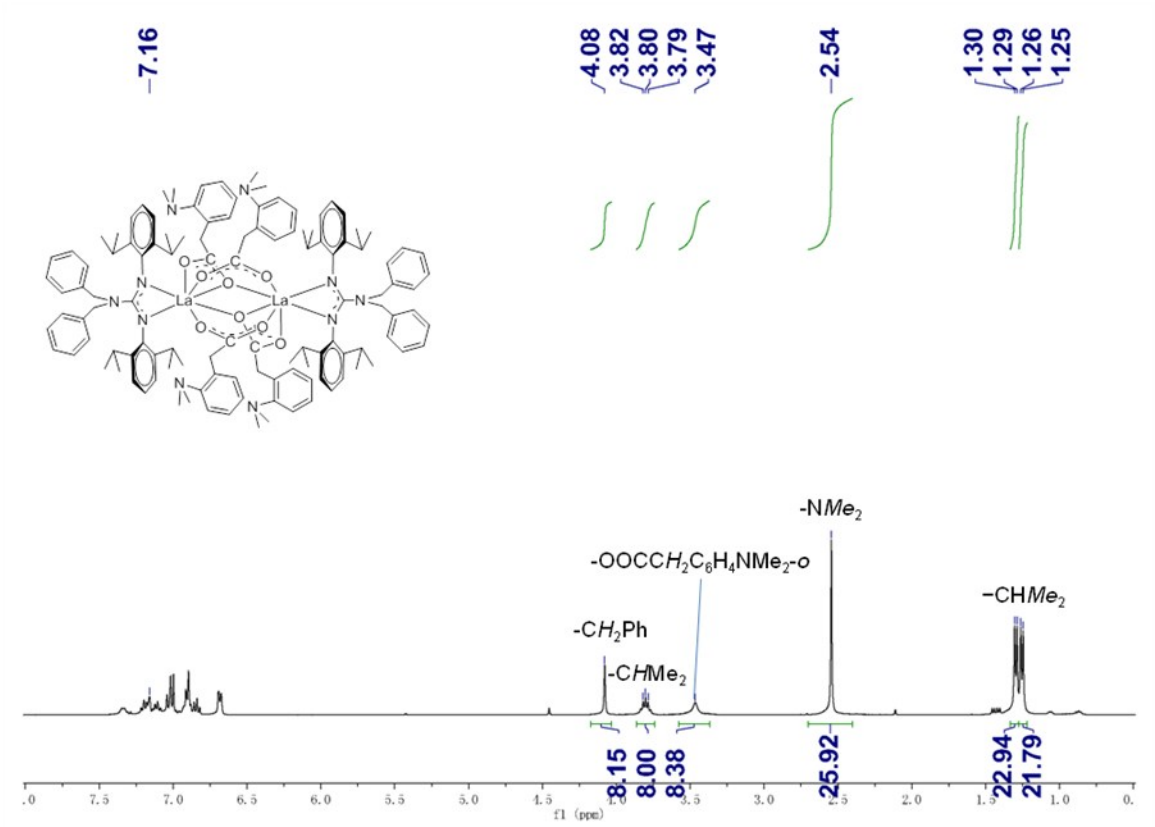

Figure S13. ^{1}H NMR spectrum of **3b** obtained in C_6D_6 at room temperature.

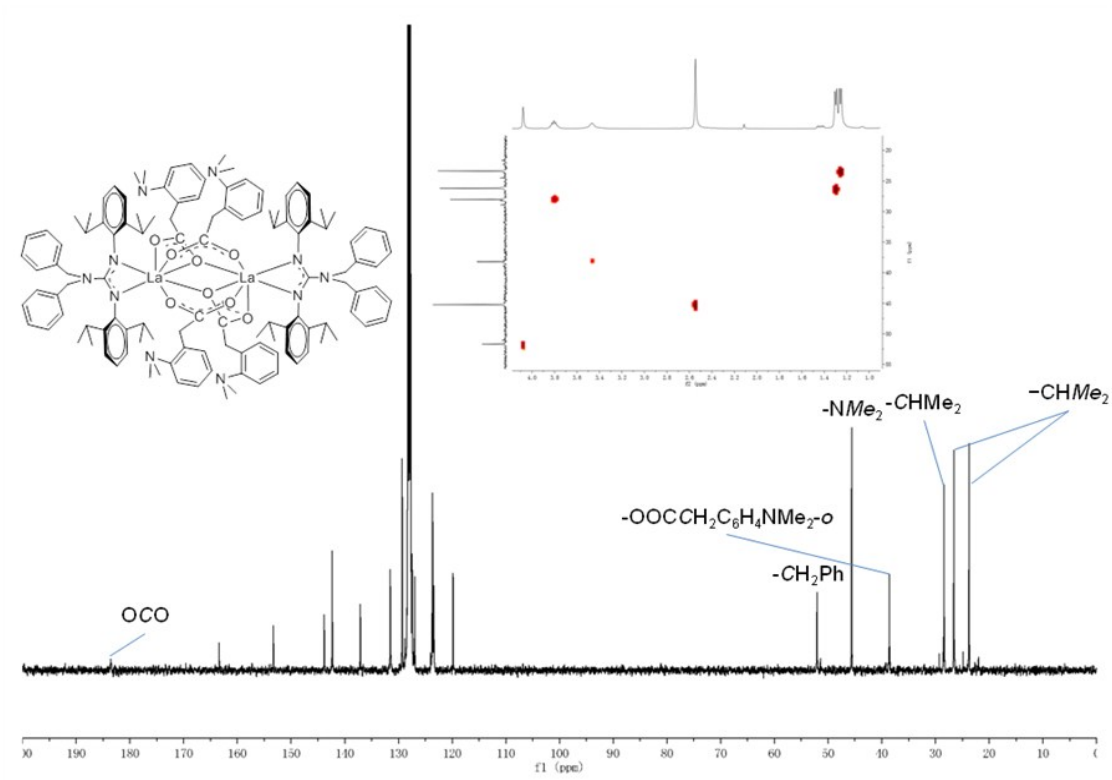

Figure S14. ^{13}C NMR spectrum of **3b** obtained in C_6D_6 at room temperature.

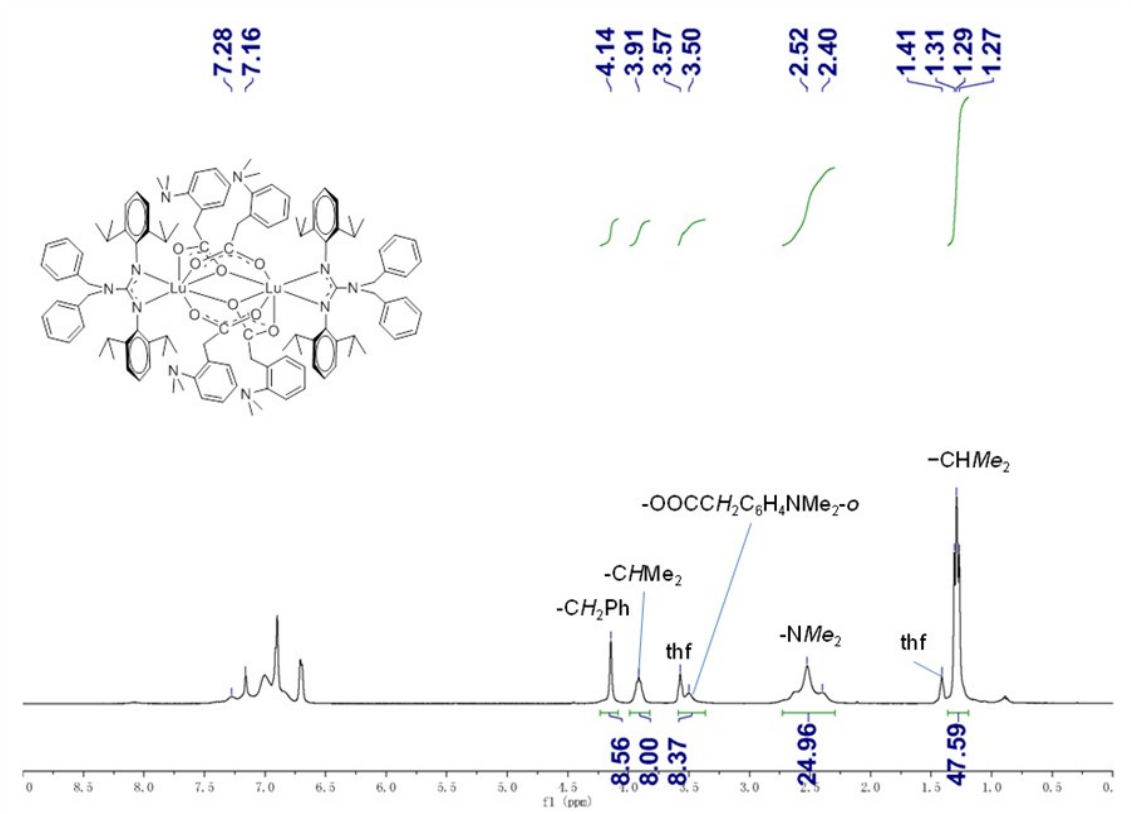

Figure S15. ^{1}H NMR spectrum of **3d** obtained in C_6D_6 at room temperature.

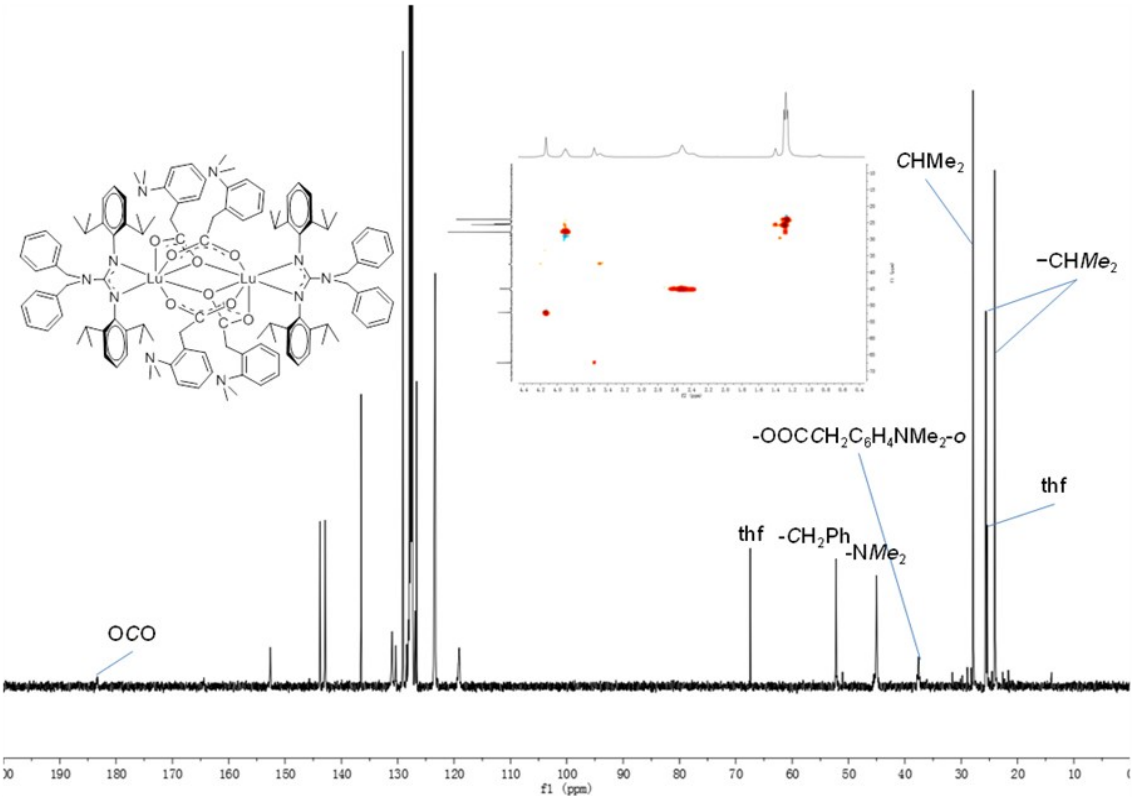

Figure S16. ^{13}C NMR spectrum of **3d** obtained in C_6D_6 at room temperature.

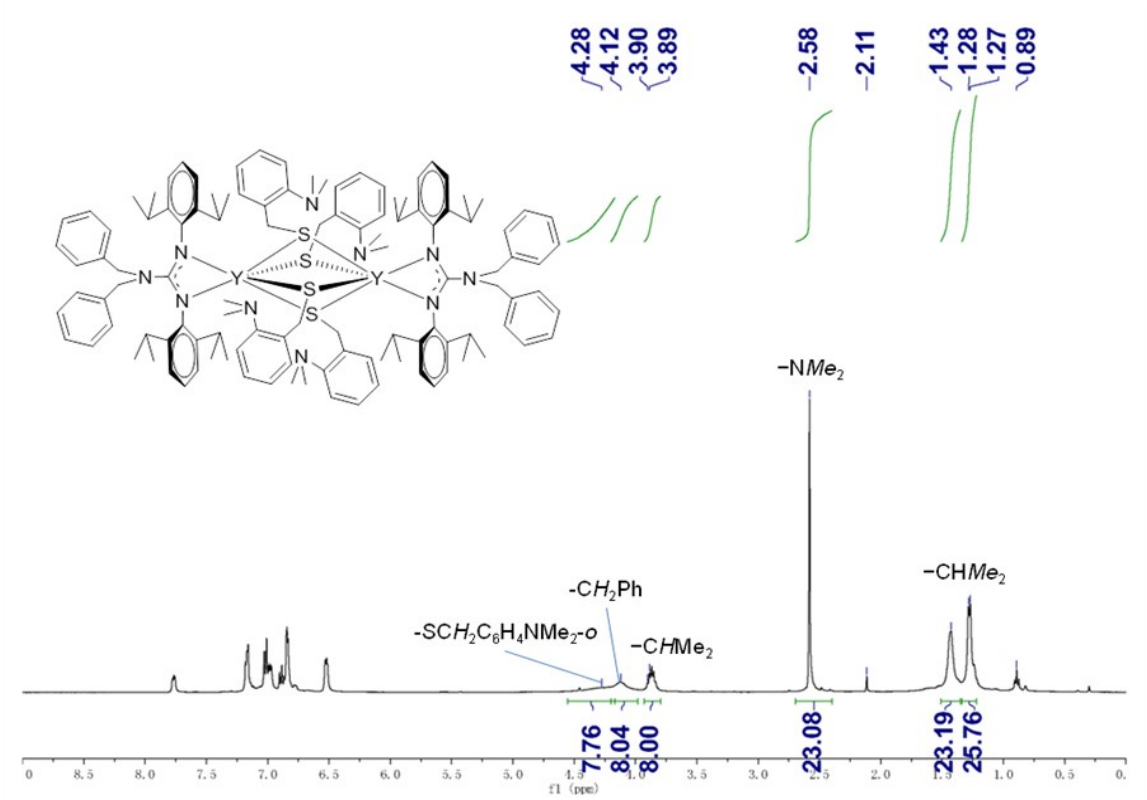

Figure S17. ^{1}H NMR spectrum of **4a** obtained in C_6D_6 at room temperature.

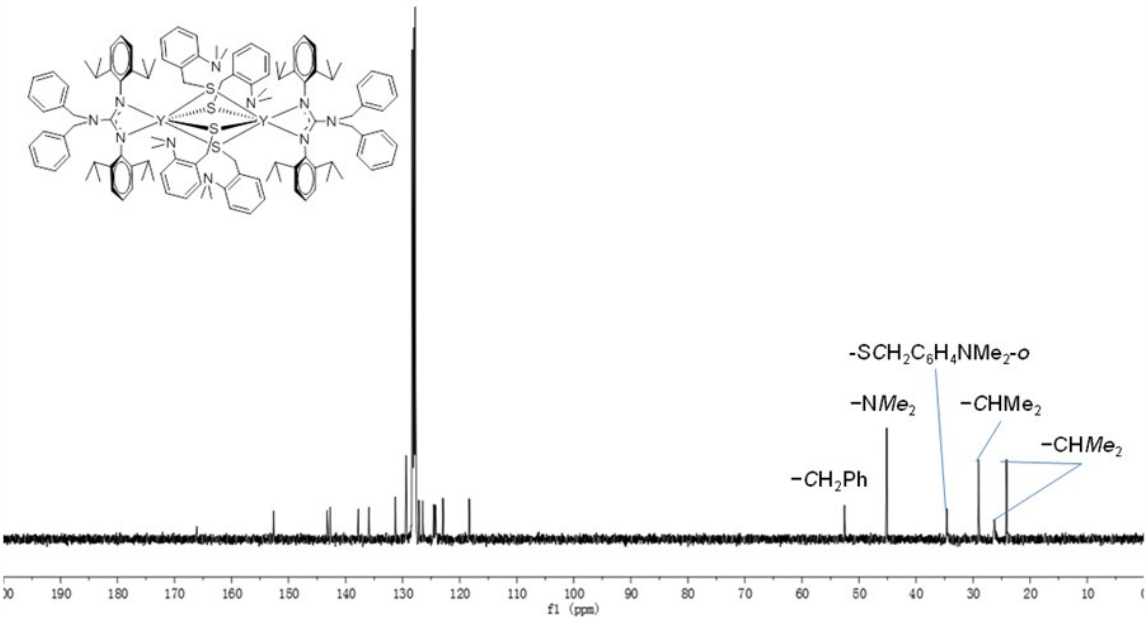

Figure S18. ^{1}H NMR spectrum of **4a** obtained in C_6D_6 at room temperature.

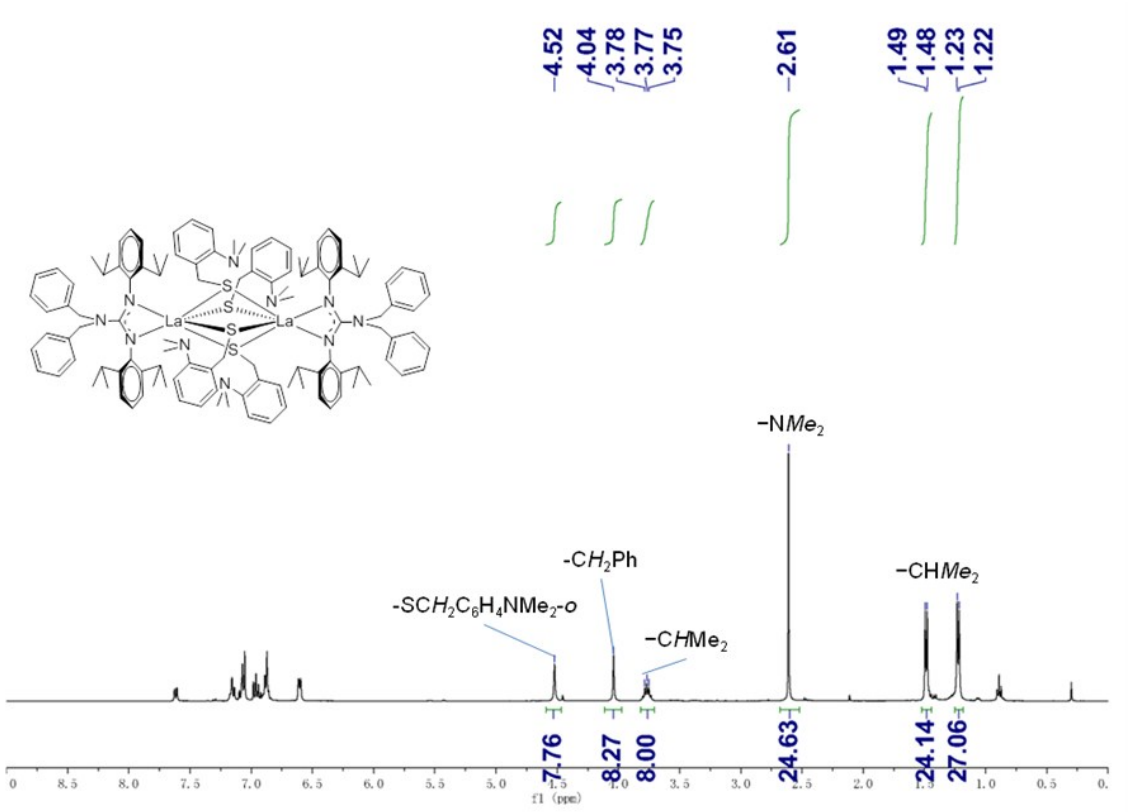

Figure S19. ^{1}H NMR spectrum of **4b** obtained in C_6D_6 at room temperature.

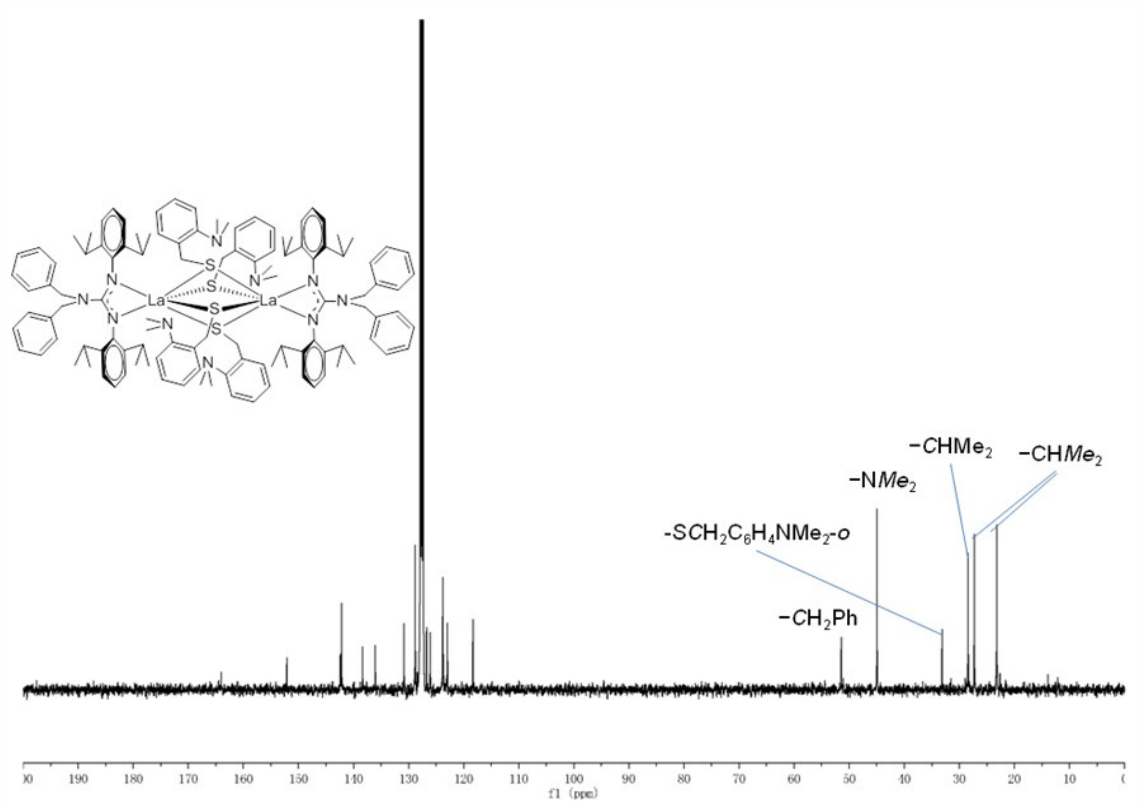

Figure S20. ^{13}C NMR spectrum of **4b** obtained in C_6D_6 at room temperature.

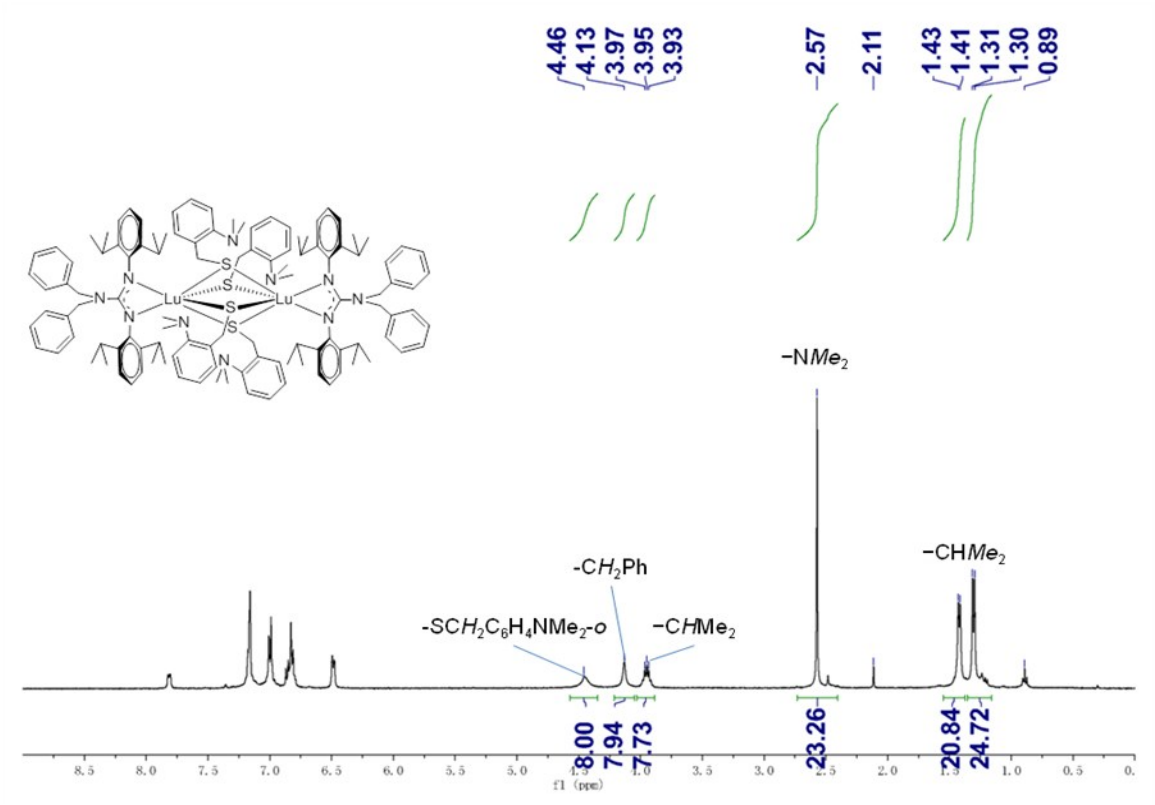

Figure S21. ^{1}H NMR spectrum of **4d** obtained in C_6D_6 at room temperature.

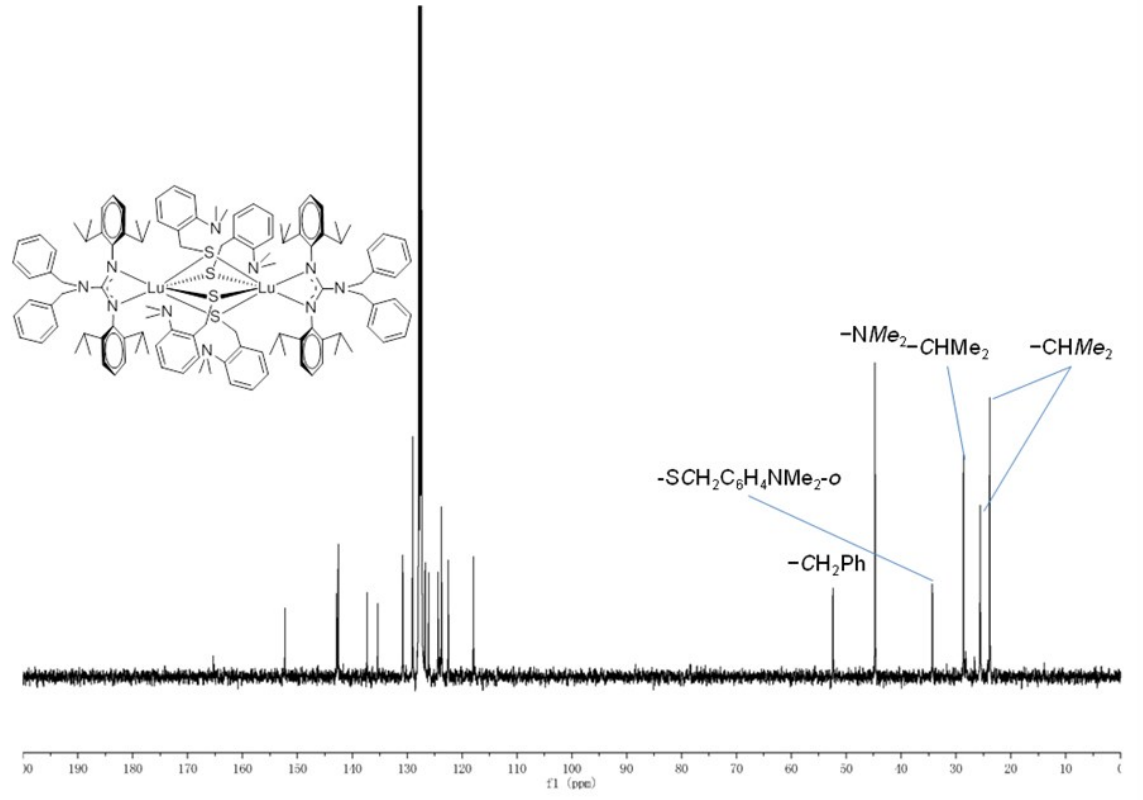

Figure S22. ^{13}C NMR spectrum of **4d** obtained in C_6D_6 at room temperature.

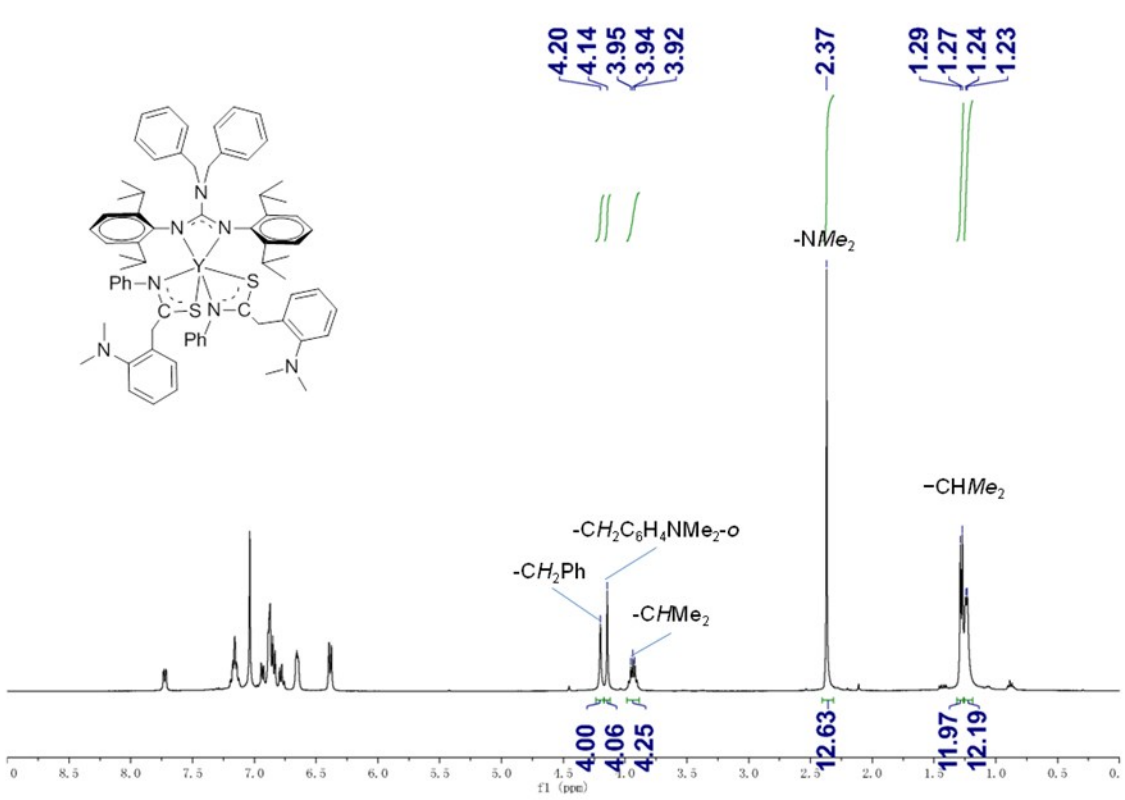

Figure S23. ^{1}H NMR spectrum of **5a** obtained in C_6D_6 at room temperature.

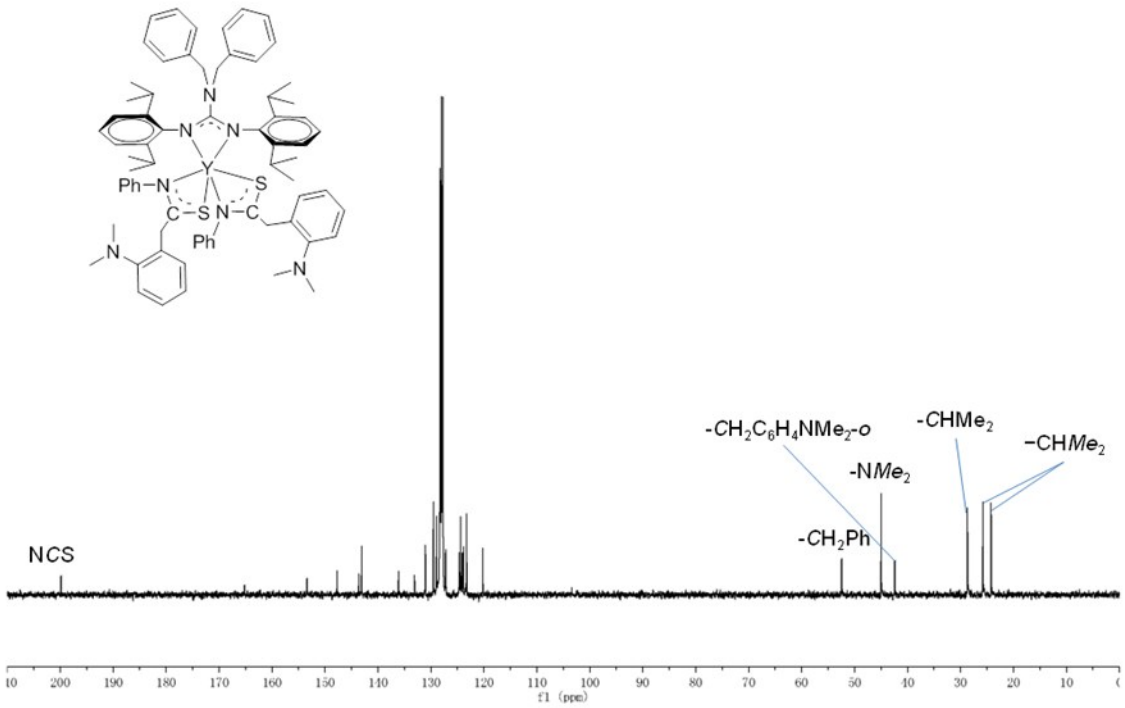

Figure S24. ^{13}C NMR spectrum of **5a** obtained in C_6D_6 at room temperature.

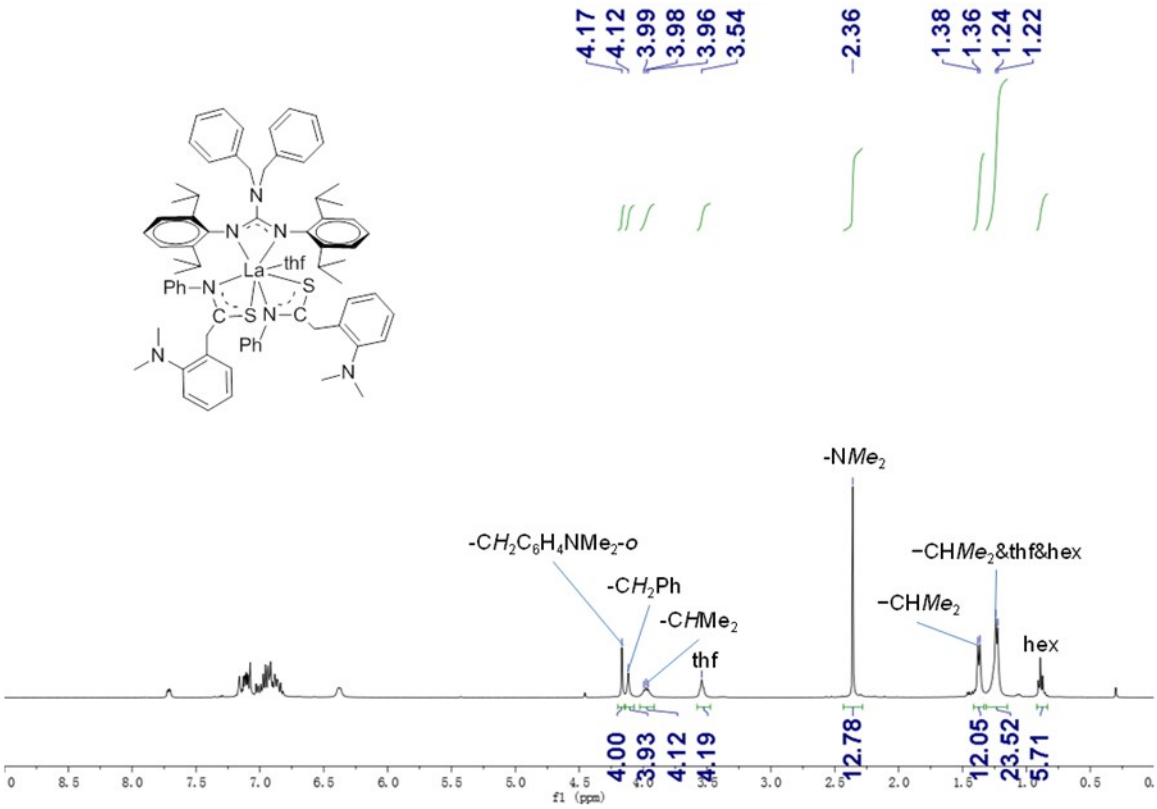

Figure S25. ^{1}H NMR spectrum of **5b** obtained in C_6D_6 at room temperature.

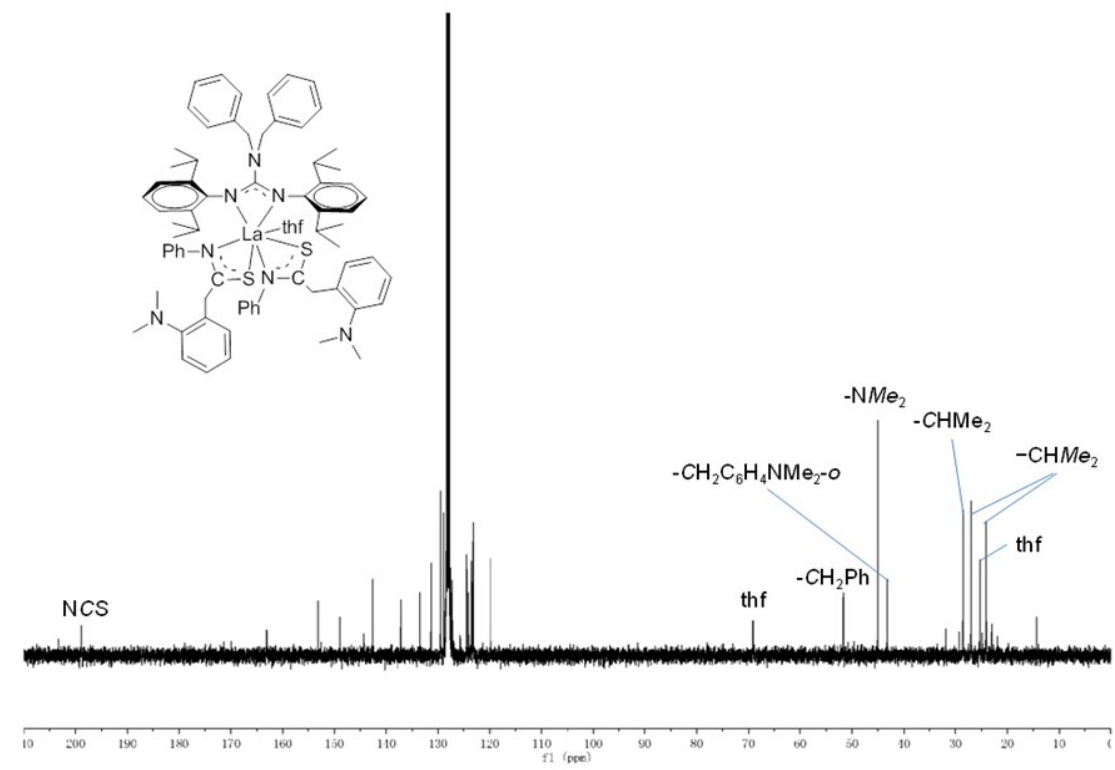

Figure S26. ^{13}C NMR spectrum of **5b** obtained in C_6D_6 at room temperature.

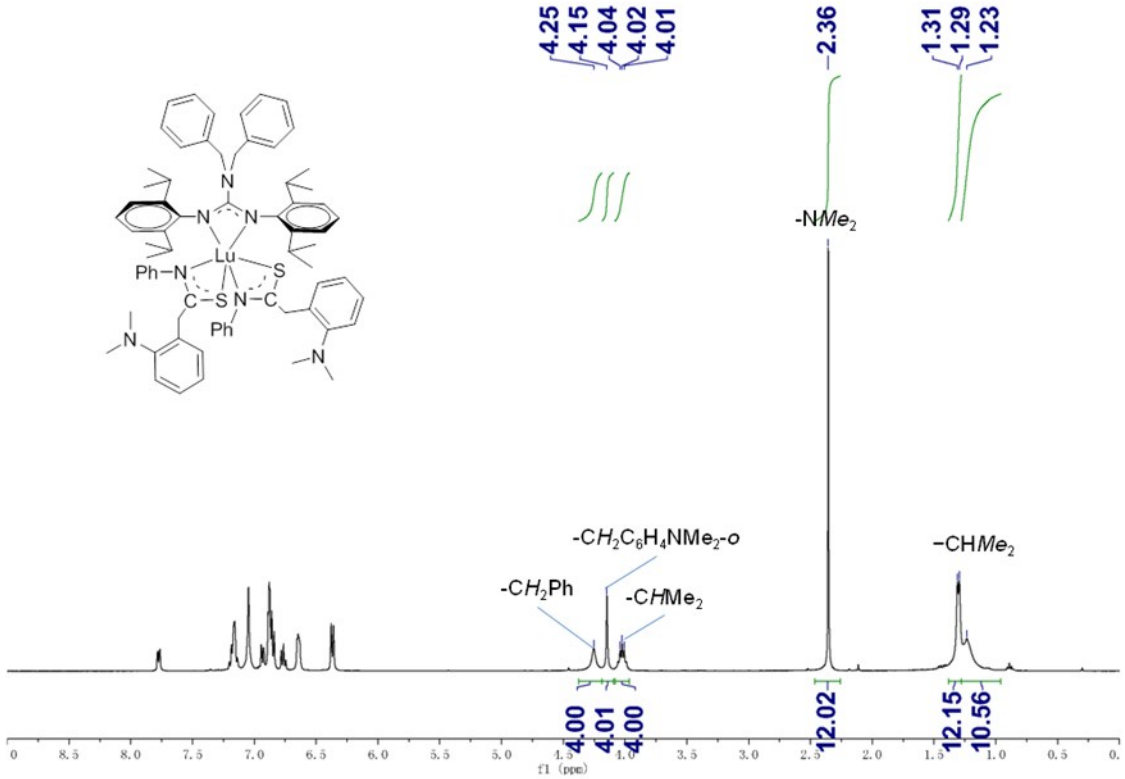

Figure S27. ^{1}H NMR spectrum of **5d** obtained in C_6D_6 at room temperature.

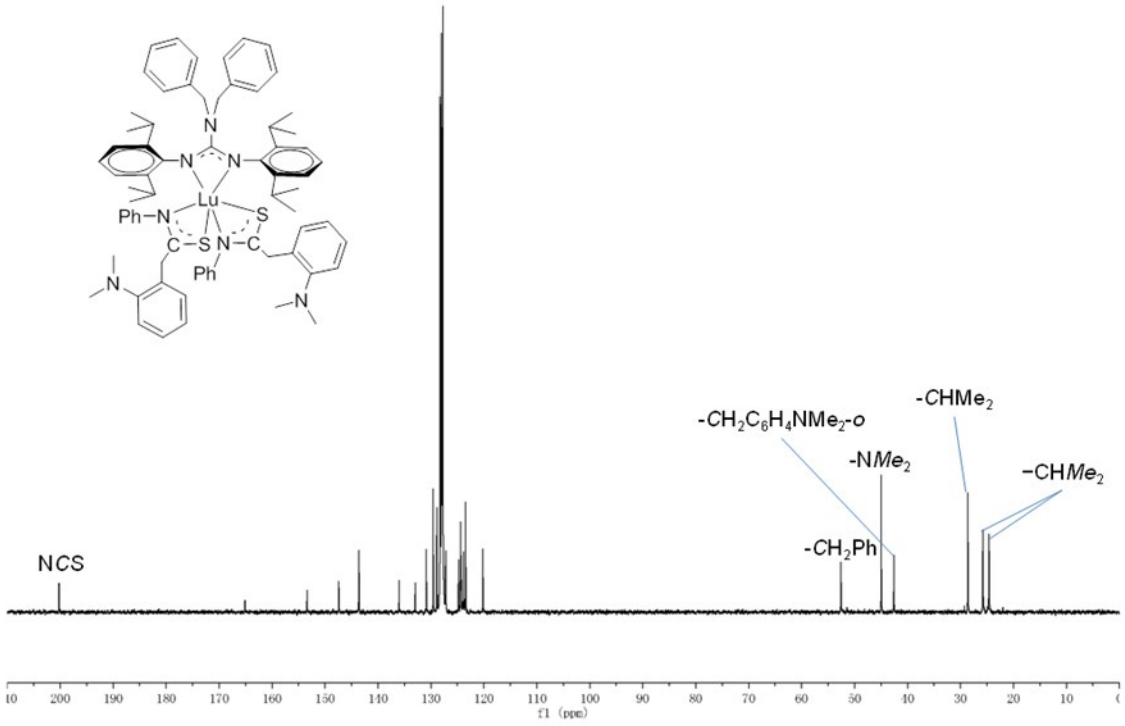

Figure S28. ^{13}C NMR spectrum of **5d** obtained in C_6D_6 at room temperature.

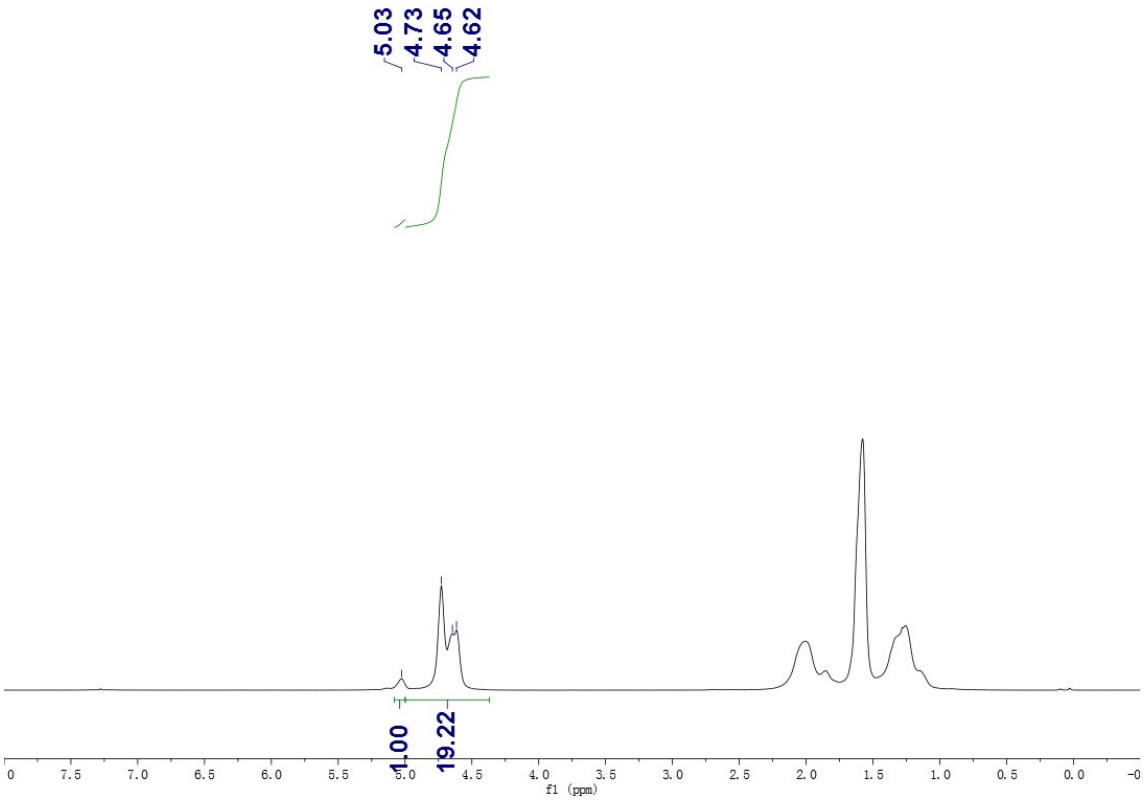

Figure S29. ^{1}H NMR spectrum of PIP obtained by complex **2a**/[Ph_3C][$B(C_6F_5)_4$] binary system at 25 ^{o}C (Table 1, Entry 1)

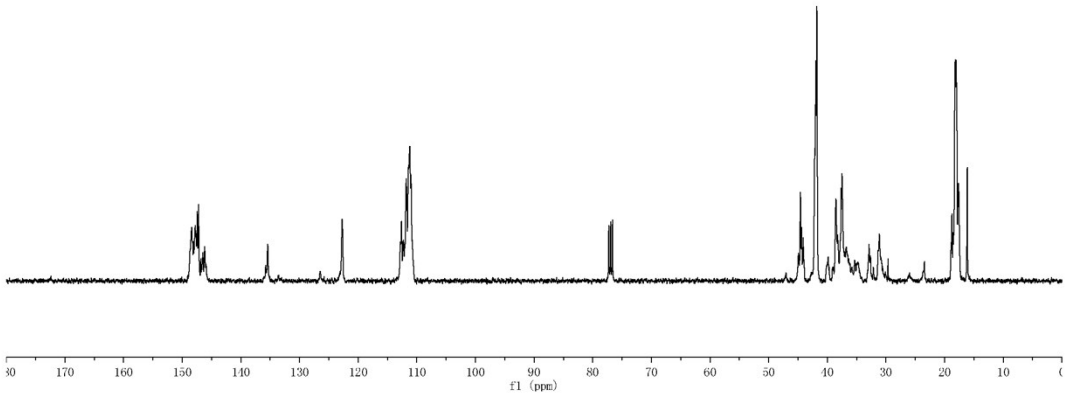

Figure S30. ^{13}C NMR spectrum of PIP obtained by complex **2a**/[Ph_3C][$B(C_6F_5)_4$] binary system at 25 ^{o}C (Table 1, Entry 1)

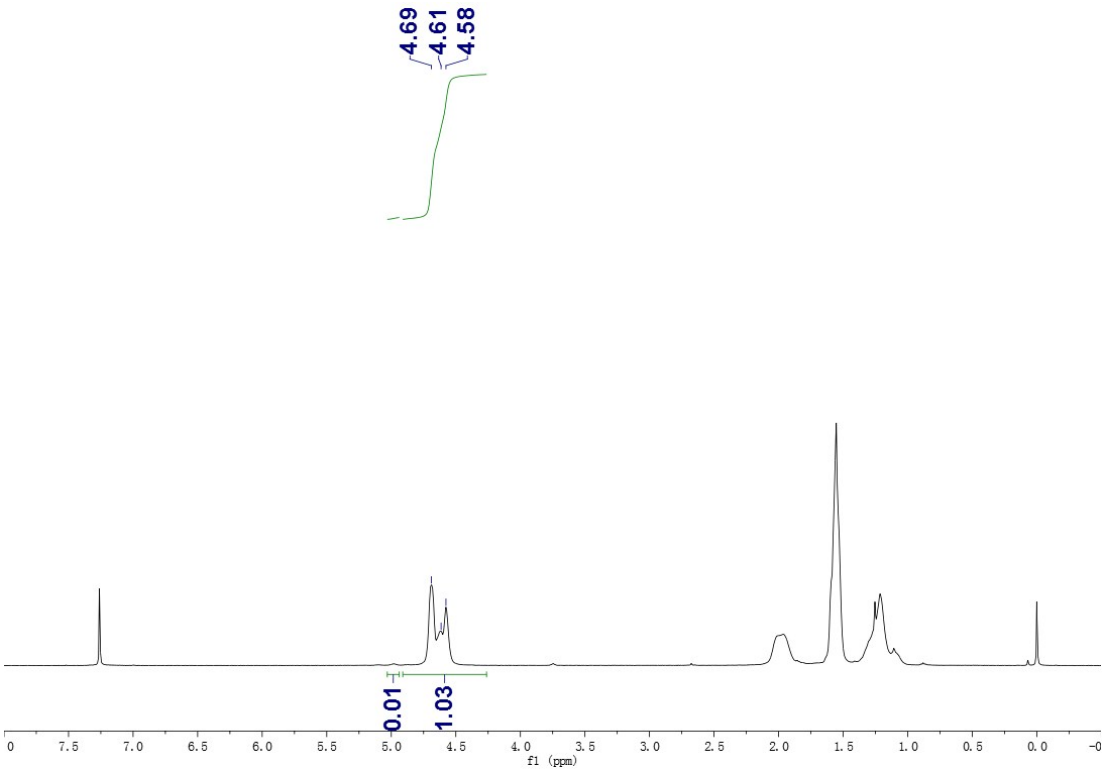

Figure S31. ^{1}H NMR spectrum of PIP obtained by complex **2a**/[Ph_3C][$B(C_6F_5)_4$] binary system at -20 ^{o}C (Table 1, Entry 10)

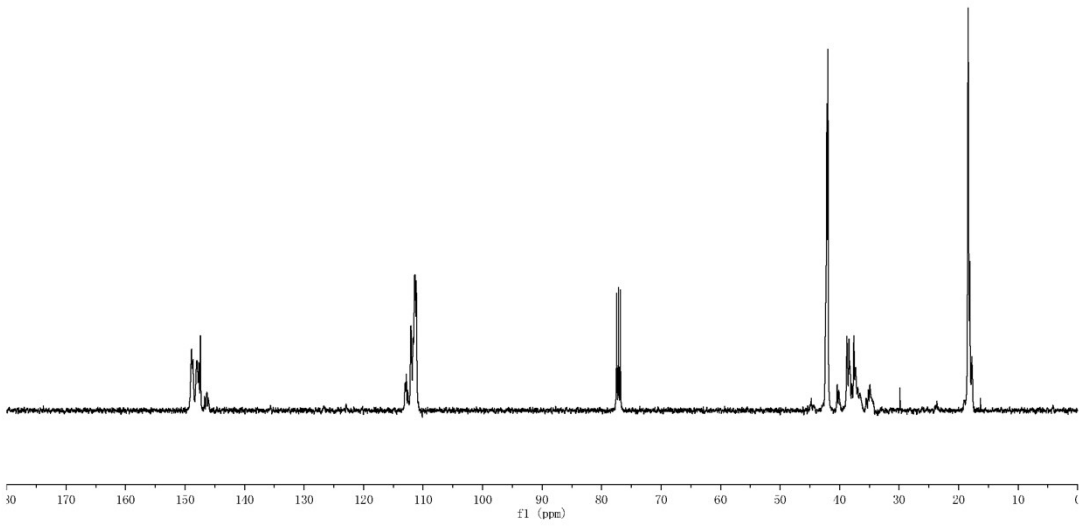

Figure S32. ^{13}C NMR spectrum of PIP obtained by complex **2a**/[Ph_3C][$B(C_6F_5)_4$] binary system at -20 ^{o}C (Table 1, Entry 10)

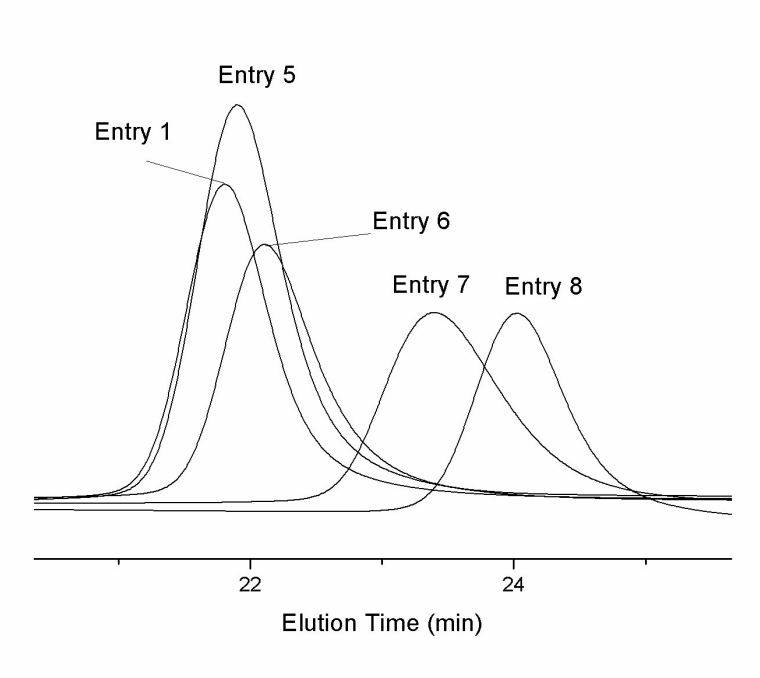

Figure S33. GPC curves of the PIP obtained by the complex **2a** at 25 °C (Table 1, Entries 1 and 5-8).

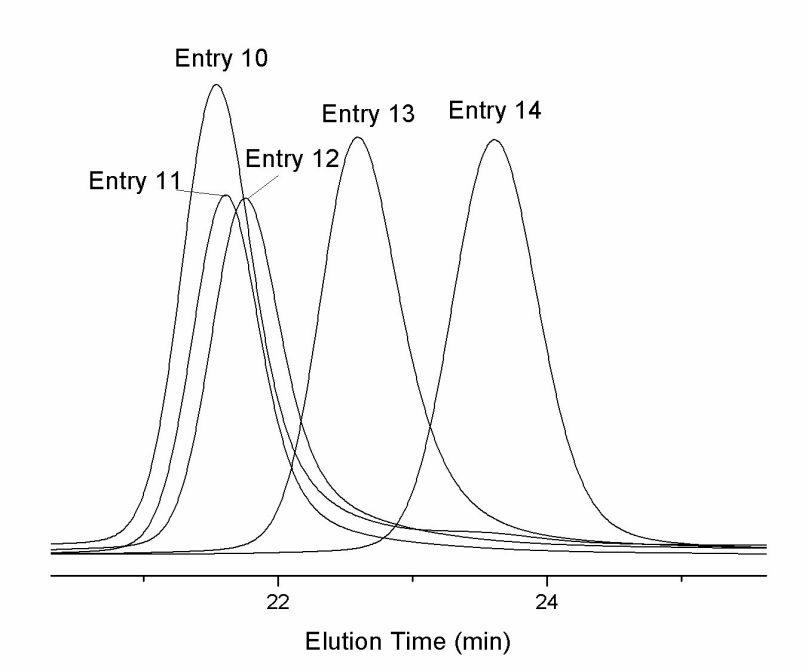

Figure S34. GPC curves of the PIP obtained by the complex **2a** at -20 °C (Table 1, Entries 1 and 10-14).

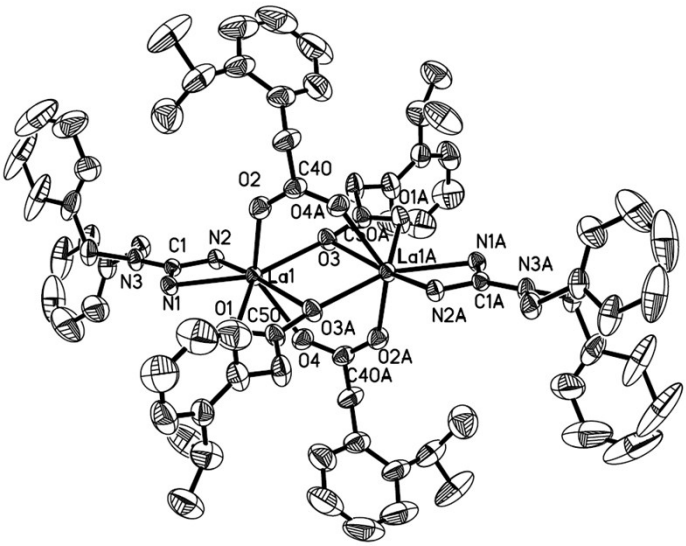

Figure S35. Molecular structure of complex **3b** with thermal ellipsoids at 30% probability. 2,6-Diisopropylphenyl groups of guanidinate ligand and all of the hydrogen atoms are omitted for clarity. Selected bond distances(Å) and angles(◦): La(1)-O(4) 2.404(3), N(1)-C(1) 1.347(4), La(1)-O(2) 2.419(3), N(2)-C(1) 1.340(4), La(1)-O(3) 2.447(2), N(3)-C(1) 1.375(4), La(1)-O(1) 2.478(2), O(1)-C(50) 1.237(4), La(1)-O(3A) 2.803(3), O(3A)-C(50) 1.272(4), La(1)-N(1) 2.496(3), O(2)-C(40) 1.256(5), La(1)-N(2) 2.500(2), O(4A)-C(40) 1.260(5); O(4)-La(1)-O(2) 137.40(9), O(4)-La(1)-O(3) 74.65(9), O(2)-La(1)-O(3) 77.83(9), O(4)-La(1)-O(1) 84.07(10), O(2)-La(1)-O(1) 90.10(10), N(1)-La(1)-N(2) 52.83(8), N(2)-C(1)-N(1) 111.6(3), O(1)-C(50)-O(3A) 120.4(3), O(2)-C(40)-O(4A) 123.0(3).

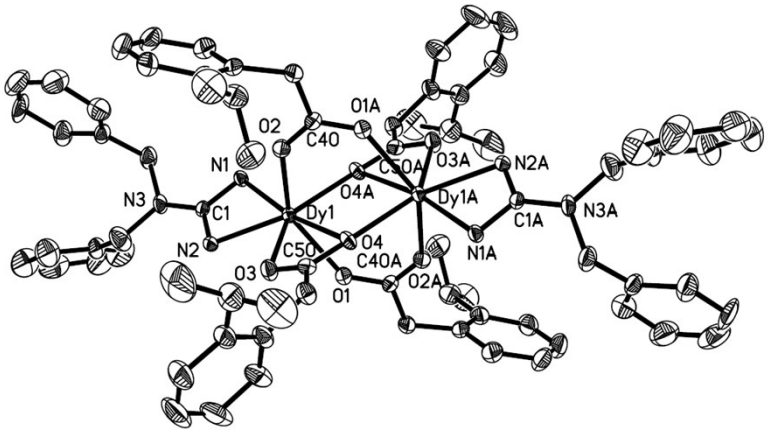

Figure S36. Molecular structure of complex **3c** with thermal ellipsoids at 30% probability. 2,6-Diisopropylphenyl groups of guanidinate ligand and all of the hydrogen atoms are omitted for clarity. Selected bond distances(Å) and angles(◦): Dy(1)-O(1) 2.300(3), N(1)-C(1) 1.341(5), Dy(1)-O(2) 2.288(3), N(2)-C(1) 1.329(5), Dy(1)-O(3) 2.334(3), N(3)-C(1) 1.384(5), Dy(1)-O(4) 2.744(3), O(1A)-C(40) 1.268(5), Dy(1)-O(4A) 2.271(3), O(2)-C(40) 1.257(5), Dy(1)-N(2) 2.333(3), O(3)-C(50) 1.231(5), Dy(1)-N(1) 2.372(3), O(4)-C(50) 1.285(5); O(2)-Dy(1)-O(1) 141.18(10), O(4A)-Dy(1)-O(4) 84.93(9), O(4A)-Dy(1)-O(2) 82.46(10), O(4A)-Dy(1)-O(1)

76.87(10), O(2)-Dy(1)-O(3) 85.73(11), N(2)-Dy(1)-N(1) 55.91(11), N(2)-C(1)-N(1) 111.4(3), O(2)-C(40)-O(1A) 123.8(4), O(3)-C(50)-O(4) 120.2(4).

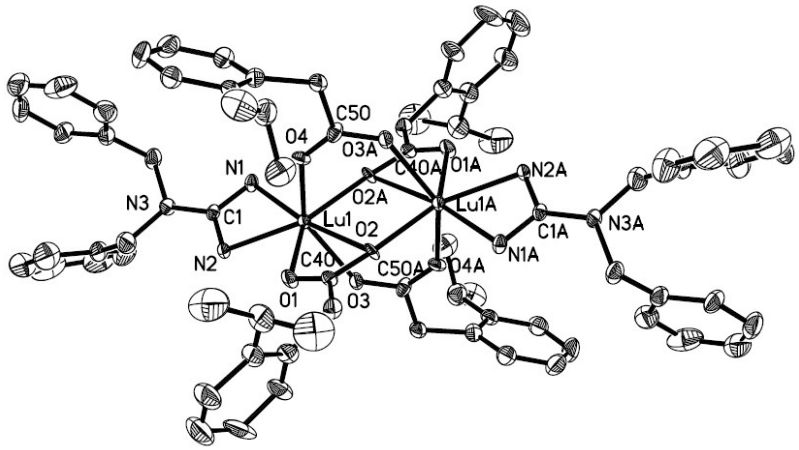

Figure S37. Molecular structure of complex **3d** with thermal ellipsoids at 30% probability. 2,6-Diisopropylphenyl groups of guanidinate ligand and all of the hydrogen atoms are omitted for clarity. Selected bond distances(Å) and angles(◦): Lu(1)-O(2A) 2.205(4), N(1)-C(1) 1.287(9), Lu(1)-O(3) 2.234(5), N(2)-C(1) 1.329(9), Lu(1)-O(4) 2.238(4), N(3)-C(1) 1.401(8), Lu(1)-O(1) 2.268(5), O(1)-C(40) 1.222(9), Lu(1)-O(2) 2.762(5), O(2)-C(40) 1.309(8), Lu(1)-N(2) 2.294(5), O(3)-C(50A) 1.273(8), Lu(1)-N(1) 2.318(5), O(4)-C(50) 1.246(9); O(3)-Lu(1)-O(4) 140.51(17), O(2A)-Lu(1)-O(2) 85.33(16), O(2A)-Lu(1)-O(1) 135.47(18), O(4)-Lu(1)-O(1) 84.83(19), O(1)-Lu(1)-O(2) 50.18(15), N(2)-Lu(1)-N(1) 55.8(2), N(1)-C(1)-N(2) 111.1(6), O(1)-C(40)-O(2) 118.8(6), O(4)-C(50)-O(3A) 122.8(6).

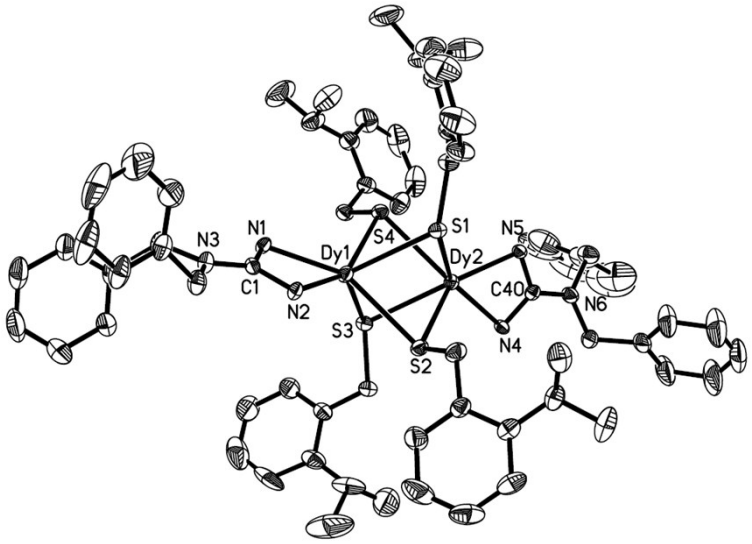

Figure S38. Molecular structure of complex **4c** with thermal ellipsoids at 30% probability. 2,6-Diisopropylphenyl groups of guanidinate ligand and all of the hydrogen atoms are omitted for clarity. Selected bond distances(Å) and angles(◦): Dy(1)-N(2) 2.321(3), Dy(2)-S(4)

2.7896(11), Dy(1)-N(1) 2.327(3), Dy(2)-S(1) 2.8070(11), Dy(1)-S(1) 2.7915(11), Dy(2)-S(2) 2.8071(11), Dy(1)-S(2) 2.7980(11), N(1)-C(1) 1.363(5), Dy(1)-S(4) 2.8069(11), N(2)-C(1) 1.354(5), Dy(1)-S(3) 2.8422(11), N(3)-C(1) 1.363(5), Dy(2)-N(5) 2.323(3), N(4)-C(40) 1.340(5), Dy(2)-N(4) 2.348(3), N(5)-C(40) 1.374(5), Dy(2)-S(3) 2.7743(11), N(6)-C(40) 1.355(5); N(2)-Dy(1)-N(1) 56.80(11), S(1)-Dy(1)-S(2) 69.39(3), S(2)-Dy(1)-S(4) 106.14(3), N(5)-Dy(2)-N(4) 56.73(11), S(1)-Dy(2)-S(2) 69.04(3), S(4)-Dy(2)-S(2) 106.37(3), Dy(1)-S(1)-Dy(2) 73.78(3), Dy(1)-S(2)-Dy(2) 73.68(3), Dy(2)-S(3)-Dy(1) 73.49(3), Dy(2)-S(4)-Dy(1) 73.81(3), N(2)-C(1)-N(1) 108.9(3), N(4)-C(40)-N(5) 109.7(4).

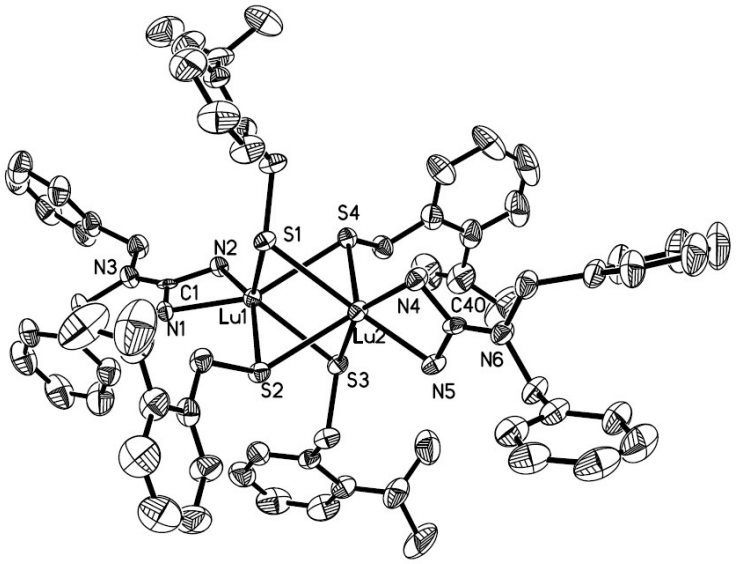

Figure S39. Molecular structure of complex **4d** with thermal ellipsoids at 30% probability. 2,6-Diisopropylphenyl groups of guanidinate ligand and all of the hydrogen atoms are omitted for clarity. Selected bond distances(Å) and angles(◦): Lu(1)-N(2) 2.251(3), Lu(2)-S(2) 2.7483(11), Lu(1)-N(1) 2.268(3), Lu(2)-S(1) 2.7722(11), Lu(1)-S(1) 2.6988(11), Lu(2)-S(3) 2.7792(11), Lu(1)-S(3) 2.7180(11), N(1)-C(1) 1.380(5), Lu(1)-S(2) 2.7612(11), N(2)-C(1) 1.398(5), Lu(1)-S(4) 2.7677(11), N(3)-C(1) 1.310(5), Lu(2)-N(4) 2.256(3), N(4)-C(40) 1.374(5), Lu(2)-N(5) 2.287(3), N(5)-C(40) 1.369(5), Lu(2)-S(4) 2.7470(12), N(6)-C(40) 1.344(5); N(2)-Lu(1)-N(1) 58.53(12), S(1)-Lu(1)-S(3) 109.55(3), S(1)-Lu(1)-S(2) 69.36(3), N(4)-Lu(2)-N(5) 58.18(12), S(4)-Lu(2)-S(2) 108.52(3), S(4)-Lu(2)-S(1) 69.34(3), Lu(1)-S(1)-Lu(2) 72.57(3), Lu(2)-S(2)-Lu(1) 72.00(3), Lu(1)-S(3)-Lu(2) 72.18(3), Lu(2)-S(4)-Lu(1) 71.92(3), N(1)-C(1)-N(2) 105.3(3), N(5)-C(40)-N(4) 107.3(4).

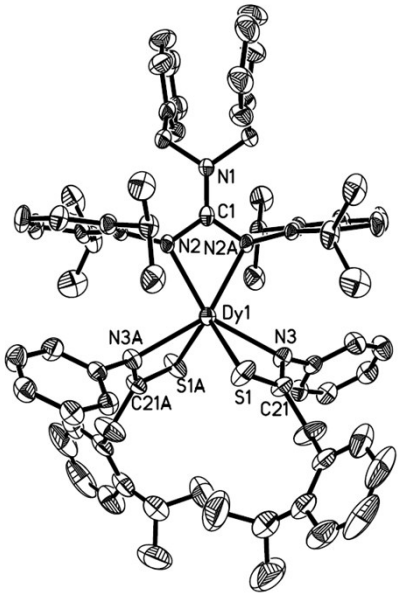

Figure S40. Molecular structure of complex **5c** with thermal ellipsoids at 30% probability. All of the hydrogen atoms are omitted for clarity. Selected bond distances(Å) and angles(◦): Dy(1)-N(2/2A) 2.335(5), Dy(1)-N(3/3A) 2.430(5), Dy(1)-S(1/1A) 2.7221(19), S(1)-C(21) 1.752(6), N(2/2A)-C(1) 1.359(7), N(1)-C(1) 1.365(12), N(3)-C(21) 1.270(8); N(2)-Dy(1)-N(2A) 56.9(2), N(2A)-C(1)-N(2) 109.8(8), N(3)-Dy(1)-S(1) 60.37(12), N(3)-C(21)-S(1) 118.0(5), C(21)-S(1)-Dy(1) 78.2(2), C(21)-N(3)-Dy(1) 99.5(4).

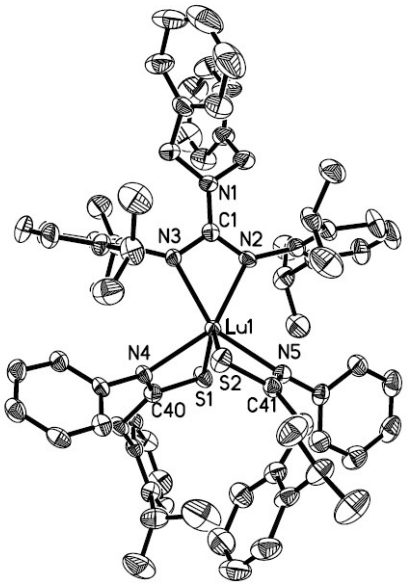

Figure S41. Molecular structure of complex **5d** with thermal ellipsoids at 30% probability. All of the hydrogen atoms are omitted for clarity. Selected bond distances(Å) and angles(◦): Lu(1)-N(3) 2.265(5), Lu(1)-N(2) 2.286(5), Lu(1)-N(4) 2.321(5), Lu(1)-N(5) 2.350(5), Lu(1)-S(1) 2.6731(19), Lu(1)-S(2) 2.6828(18), S(1)-C(40) 1.726(6), S(2)-C(41) 1.722(6), N(1)-C(1) 1.397(8), N(4)-C(40) 1.293(8), N(5)-C(41) 1.307(7); N(3)-Lu(1)-N(2) 57.80(16), N(5)-Lu(1)-S(2) 61.90(11),

N(3)-Lu(1)-N(4) 94.60(17), S(1)-Lu(1)-S(2) 130.36(6), N(2)-Lu(1)-N(4) 142.84(18), C(40)-S(1)-Lu(1) 78.0(2), N(3)-Lu(1)-N(5) 148.12(19), C(41)-S(2)-Lu(1) 78.8(2), N(2)-Lu(1)-N(5) 100.47(17), C(1)-N(2)-Lu(1) 95.2(3), N(4)-Lu(1)-N(5) 113.87(18), C(1)-N(3)-Lu(1) 95.0(3), N(3)-Lu(1)-S(1) 115.43(13), C(40)-N(4)-Lu(1) 101.1(4), N(2)-Lu(1)-S(1) 104.74(13), C(41)-N(5)-Lu(1) 100.6(4), N(4)-Lu(1)-S(1) 62.35(12), N(2)-C(1)-N(3) 112.1(5), N(5)-Lu(1)-S(1) 91.40(13), N(2)-C(1)-N(1) 124.9(5), N(3)-Lu(1)-S(2) 106.39(12), N(3)-C(1)-N(1) 123.0(5), N(2)-Lu(1)-S(2) 120.03(13), N(4)-C(40)-S(1) 118.4(5), N(4)-Lu(1)-S(2) 89.70(13), N(5)-C(41)-S(2) 117.9(5).

Table S1. Crystal data and refinement details of complexes **1,3b-d**

	1	**3b**	**3c**	**3d**
Formula	$C_{39}H_{48}N_3$	$C_{59}H_{72}N_5O_4La$	$C_{59}H_{72}N_5O_4Dy$	$C_{59}H_{72}N_5O_4Lu$
Formula weight	558.80	1054.13	1077.71	1090.18
Temperature (K)	293(2)	273(2)	273(2)	296(2)
Wavelength(Å)	0.71073	0.71073	0.71073	0.71073
Crystal system	Triclinic	Monoclinic	Triclinic	Triclinic
space group	P-1	P2(1)/n	P-1	P-1
a(Å)	10.323(8)	17.229(2)	13.052(3)	13.0131(13)
b(Å)	10.930(8)	16.7584(19)	16.105(3)	16.0451(16)
c(Å)	16.132(12)	20.095(2)	16.969(6)	16.917(3)
α(°)	79.031(7)	90	103.980(3)	103.838(2)
β(°)	82.038(9)	107.6720	104.552(3)	104.826(2)
γ(°)	82.388(9)	90	112.507(2)	112.459(2)
V (Å^3)	1759(2)	5528.3(11)	2953.3(13)	2922.6(6)
Z	2	4	2	2
D_c (g/cm^3)	1.055	1.267	1.212	1.239
μ (mm^{-1})	0.061	0.82	1.310	1.735
F(000)	606	2200	1118	1128
Crystal size (mm^3)	0.40x0.40x0.10	0.40x0.32x0.26	0.42x0.38x0.35	0.50x0.48x0.43
θ range (°)	1.295 to 25.050	1.37 to 25.05	1.339 to 25.05	1.483 to 25.049
h, k, l range	-6<=h<=12, -12<=k<=13, -19<=l<=19	-20<=h<=20 -19<=k<=19 -14<=l<=23	-15<=h<=14 -19<=k<=19 -20<=l<=19	-15<=h<=15 -19<=k<=19 -20<=l<=13
Reflections collected	8582	26960	14407	17550
Reflections unique	6058 [R(int)=0.0235]	9767 [R(int)=0.0259]	10192 [R(int) = 0.0238]	10217 [R(int) = 0.0305]
Completeness to θ	97.2 % (θ = 25.05)	99.8 % (θ = 25.05)	97.4 %(θ = 25.05)	98.7 %(θ = 25.049)
Max. and min. Transmission	0.7455 and 0.6045	0.8148 and 0.7347	0.7456 and 0.4990	0.7455 and 0.4760
Refinement method	Full-matrix least-squares on F^2	Full-matrix least-squares on F^2	Full-matrix least-squares on F^2	Full-matrix least-squares on F^2
Data / restraints / parameters	6058 / 0 / 388	9767 / 0 / 622	10192 / 0 / 634	10217 / 0 / 634
Goodness-of-fit on F^2	1.047	1.051	0.983	1.032
Final *R* indices [$I>2\sigma(I)$]	R_1 = 0.0618, wR_2 = 0.1760	R_1 = 0.0379, wR_2 = 0.1046	R_1 = 0.0349, wR_2 = 0.0916	R_1 = 0.0468, wR_2 = 0.1399
R indices (all data)	R_1 = 0.0877, wR_2 = 0.1995	R_1 = 0.0549, wR_2 = 0.1213	R_1 = 0.0454, wR_2 = 0.0940	R_1 = 0.0587, wR_2 = 0.1774
Largest diff. peak and hole (e Å^{-3})	0.508 and -0.264	0.906 and -0.462	1.004 and -0.697	1.524 and -1.852

Table S2. Crystal data and refinement details of complexes **4c**, **4d, 5c, 5d**

	4c	**4d**	**5c**	**5d**
Formula	$C_{114}H_{144}N_{10}S_4Dy_2$	$C_{114}H_{144}N_{10}S_4Lu_2$	$C_{71}H_{82}N_7S_2Dy$	$C_{71}H_{82}N_7S_2Lu$
Formula weight	2107.63	2132.57	1260.06	1272.53
Temperature (K)	273(2)	273(2)	273(2)	293(2)
Wavelength(Å)	0.71073	0.71073	0.71073	0.71073
Crystal system	Monoclinic	Triclinic	Monoclinic	Triclinic
space group	P2(1)/n	P-1	C2/c	P-1
a (Å)	15.4557(17)	14.1932(16)	13.114(3)	10.950(4)
b (Å)	23.843(3)	15.3802(18)	26.401(6)	14.310(5)
c (Å)	31.373(4)	30.149(4)	19.568(5)	22.145(7)
α (deg)	90	94.987(2)	90	106.075(4)
β (deg)	98.9200(10)	92.195(2)	104.312(3)	93.766(4)
γ (deg)	90	116.5510(10)	90	98.308(4)
V (Å^3)	11421(2)	5842.9(13)	6565(3)	3278.7(19)
Z	4	2	4	2
Dc (g/cm^3)	1.226	1.212	1.275	1.289
μ (mm^{-1})	1.419	1.798	1.247	1.615
F(000)	4376	2208	2620	1320
Crystal size (mm)	0.32 x 0.30 x 0.24	0.36 x 0.30 x 0.25	0.40 x 0.35 x 0.30	0.33 x 0.20 x 0.18
θ range (°)	1.08 to 25.05	1.49 to 25.05	1.54 to 25.05	1.50 to 25.05
h, k, l range	-18<=h<=16 -28<=k<=27 -37<=l<=29	-11<=h<=16 -18<=k<=18 -35<=l<=35	-13<=h<=15 -31<=k<=22 -23<=l<=23	-12<=h<=12 -17<=k<=16 -17<=l<=26
Reflections collected	56673	29365	15475	12846
Reflections unique	20182 [R(int)=0.0508]	20350 [R(int)=0.0235]	5809 [R(int)=0.0866]	10967 [R(int)=0.0249]
Completeness to *θ*	99.8 %(θ = 25.05)	98.3 %(θ = 25.05)	99.7 % (θ = 25.05)	94.8 % (θ = 25.05)
Max. and min. Transmission	0.7269 and 0.6595	0.6621 and 0.5638	0.7060 and 0.6353	0.7598 and 0.6179
Refinement method	Full-matrix least-squares on F^2	Full-matrix least-squares on F^2	Full-matrix least-squares on F^2	Full-matrix least-squares on F^2
Data / restraints / parameters	20182 / 12 / 1183	20350 / 0 / 1195	5809 / 0 / 373	10967 / 0 / 742
Goodness-of-fit on F2	1.014	1.029	1.006	1.044
Final R indices [*I>2σ(I)*]	R_1 = 0.0409, wR_2 = 0.0770	R_1 = 0.0379, wR_2 = 0.0959	R_1 = 0.0783, wR_2 = 0.1827	R_1 = 0.0405, wR_2 = 0.1294
R indices (all data)	R_1 = 0.0718, wR_2 = 0.0823	R_1 = 0.0593, wR_2 = 0.1027	R_1 = 0.0898, wR_2 = 0.1915	R_1 = 0.0530, wR_2 = 0.1465
Largest diff. peak and hole (e Å^{-3})	1.164 and -0.782	1.088 and -0.675	2.682 and -5.264	1.392 and -1.030